

2010-210 \_\_\_\_\_ BWR Vessel & Internals Project (BWRVIP)

September 15, 2010

Document Control Desk  
U. S. Nuclear Regulatory Commission  
11555 Rockville Pike  
Rockville, MD 20852

Attention: Jonathan Rowley

Subject: Project No. 704 – “BWRVIP-199NP: BWR Vessel and Internals Project, Testing and Evaluation of the Monticello 300° Capsule,”

Reference: BWRVIP letter 2009-053 from Rick Libra (BWRVIP Chairman) to Document Control Desk (NRC), “BWRVIP-199: BWR Vessel and Internals Project, Testing and Evaluation of the Monticello 300° Capsule,” dated February 19, 2009

Enclosed for your information are five (5) copies of the report “BWRVIP-199NP: BWR Vessel and Internals Project, Testing and Evaluation of the Monticello 300° Capsule,” EPRI Technical Report 1021557, August 2010. This report is a non-proprietary version of the proprietary report transmitted to the NRC staff by the BWRVIP letter referenced above. The technical content of the enclosed report is identical to that in the proprietary version transmitted to the NRC staff by the BWRVIP letter referenced above. The content was re-classified as non-proprietary and is being provided in response to a request from the NRC staff so that the data in the report can be used in the NRC public database of reactor pressure vessel embrittlement data.

Please note that the enclosed report is non-proprietary and is available to the public by request to EPRI.

If you have any questions on this subject please call Randy Schmidt (PSEG Nuclear, BWRVIP Assessment Committee Technical Chairman) at 856-339-3740.

Sincerely,



Dave Czufin  
Exelon  
Chairman, BWR Vessel and Internals Project

c: Gary Stevens, NRC  
Matt Mitchell, NRC

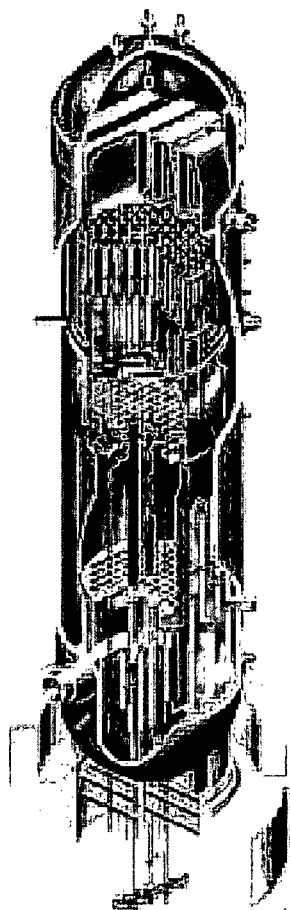
Together . . . Shaping the Future of Electricity

Additional copies  
sent to PM

Good  
NRK

# BWVRVIP-199NP: BWR Vessel and Internals Project

## Testing and Evaluation of the Monticello 300° Capsule



# **BWRVIP-199NP: BWR Vessel and Internals Project**

Testing and Evaluation of the Monticello  
300° Capsule

**1021557**

Final Report, August 2010

EPRI Project Manager  
R. Carter

Work to develop this product was completed under the EPRI Nuclear Quality Assurance Program  
in compliance with 10 CFR 50, Appendix B and 10 CFR 21,



## **DISCLAIMER OF WARRANTIES AND LIMITATION OF LIABILITIES**

THIS DOCUMENT WAS PREPARED BY THE ORGANIZATION(S) NAMED BELOW AS AN ACCOUNT OF WORK SPONSORED OR COSPONSORED BY THE ELECTRIC POWER RESEARCH INSTITUTE, INC. (EPRI). NEITHER EPRI, ANY MEMBER OF EPRI, ANY COSPONSOR, THE ORGANIZATION(S) BELOW, NOR ANY PERSON ACTING ON BEHALF OF ANY OF THEM:

(A) MAKES ANY WARRANTY OR REPRESENTATION WHATSOEVER, EXPRESS OR IMPLIED, (I) WITH RESPECT TO THE USE OF ANY INFORMATION, APPARATUS, METHOD, PROCESS, OR SIMILAR ITEM DISCLOSED IN THIS DOCUMENT, INCLUDING MERCHANTABILITY AND FITNESS FOR A PARTICULAR PURPOSE, OR (II) THAT SUCH USE DOES NOT INFRINGE ON OR INTERFERE WITH PRIVATELY OWNED RIGHTS, INCLUDING ANY PARTY'S INTELLECTUAL PROPERTY, OR (III) THAT THIS DOCUMENT IS SUITABLE TO ANY PARTICULAR USER'S CIRCUMSTANCE; OR

(B) ASSUMES RESPONSIBILITY FOR ANY DAMAGES OR OTHER LIABILITY WHATSOEVER (INCLUDING ANY CONSEQUENTIAL DAMAGES, EVEN IF EPRI OR ANY EPRI REPRESENTATIVE HAS BEEN ADVISED OF THE POSSIBILITY OF SUCH DAMAGES) RESULTING FROM YOUR SELECTION OR USE OF THIS DOCUMENT OR ANY INFORMATION, APPARATUS, METHOD, PROCESS, OR SIMILAR ITEM DISCLOSED IN THIS DOCUMENT.

THE FOLLOWING ORGANIZATION(S), UNDER CONTRACT TO EPRI, PREPARED THIS REPORT:

**ATI Consulting**

**MPM Research & Consulting**

**TransWare Enterprises Inc.**

THE TECHNICAL CONTENTS OF THIS DOCUMENT WERE PREPARED IN ACCORDANCE WITH THE EPRI QUALITY PROGRAM MANUAL THAT FULFILLS THE REQUIREMENTS OF 10 CFR 50 APPENDIX B, 10 CFR 21, ANSI N45.2-1977 AND/ OR THE INTENT OF ISO-9001 (1994).

CONTRACTUAL ARRANGEMENTS BETWEEN THE CUSTOMER AND EPRI MUST BE ESTABLISHED BEFORE QUALITY APPLICATION TO ASSURE FULFILLMENT OF QUALITY PROGRAM REQUIREMENTS.

### **NOTE**

For further information about EPRI, call the EPRI Customer Assistance Center at 800.313.3774 or e-mail [askepri@epri.com](mailto:askepri@epri.com).

Electric Power Research Institute, EPRI, and TOGETHER...SHAPING THE FUTURE OF ELECTRICITY are registered service marks of the Electric Power Research Institute, Inc.

Copyright © 2010 Electric Power Research Institute, Inc. All rights reserved.

## ACKNOWLEDGMENTS

---

The following organizations, under contract to the Electric Power Research Institute (EPRI), prepared this report:

ATI Consulting  
PO Box 5769  
Pinehurst, NC 28374

Principal Investigators  
T. Hardin

MPM Research & Consulting  
2161 Sandy Drive  
State College, PA 16803

Principal Investigator  
Dr. M. P. Manahan, Sr.

TransWare Enterprises Inc.  
1565 Mediterranean Drive  
Sycamore, IL 60178

Principal Investigators  
K. M. Retzke  
D. B. Jones

This report describes research sponsored by EPRI and its BWRVIP participating members.

---

This publication is a corporate document that should be cited in the literature in the following manner:

*BWRVIP-199NP: BWR Vessel and Internals Project: Testing and Evaluation of the Monticello 300 Capsule.* EPRI, Palo Alto, CA: 2010. 1021557.

# PRODUCT DESCRIPTION

---

In the late 1990s, a BWR Vessel and Internals Project (BWRVIP) Integrated Surveillance Program (ISP) was developed to improve the surveillance of the U.S. BWR fleet. This report describes testing and evaluation of the Monticello 300° Capsule. These results will be used to monitor embrittlement as part of the BWRVIP ISP.

## Results and Findings

The report includes specimen chemical compositions, capsule neutron exposure, and Charpy V-notch test results for Monticello surveillance plate heat C2220. The project compared irradiated Charpy data for the plate specimens to unirradiated data to determine the shift in Charpy index temperatures due to irradiation. Results indicate a shift lower than the prediction of Regulatory Guide 1.99, Revision 2. Researchers also measured flux wires and determined fluence for the capsule.

## Challenges and Objectives

Neutron irradiation exposure reduces the toughness of reactor vessel steel plates, welds, and forgings. The objectives of this project were two-fold:

- To document results of neutron dosimetry and Charpy-V notch ductility tests for the plate surveillance material C2220 in the Monticello 300° capsule.
- To compare results with the embrittlement trend prediction of the U.S. Nuclear Regulatory Commission (USNRC) Regulatory Guide 1.99, Rev. 2.

## Applications, Values, and Use

Results of this work will be used in the BWRVIP ISP that integrates individual BWR surveillance programs into a single program. The ISP provides data of high quality to monitor BWR vessel embrittlement. The ISP results in significant cost savings to the BWR fleet and provides more accurate monitoring of embrittlement in BWR vessels.

## EPRI Perspective

The BWRVIP ISP represents a major enhancement to the process of monitoring embrittlement for the U.S. fleet of BWRs. The ISP optimizes surveillance capsule tests while at the same time maximizing the quantity and quality of data, thus resulting in a more cost effective program. The BWRVIP ISP provides more representative data that may be used to assess embrittlement in RPV vessel beltline materials and improve trend curves in the BWR range of irradiation conditions.

**Approach**

The Monticello 300° capsule had been irradiated in the reactor since plant startup. The surveillance capsule contained flux wires for neutron flux monitoring, Charpy V-notch impact test specimens, and tensile specimens. The project team removed the capsule from the reactor in 2007 and transported it to facilities for testing and evaluation. The team used dosimetry to gather information about the neutron fluence accrual of specimens from the capsule. They then performed a neutron transport calculation in accordance with Regulatory Guide 1.190 and compared it to the results from the dosimetry. Testing of Charpy V-notch specimens was performed according to American Society for Testing and Materials (ASTM) standards.

**Keywords**

Reactor pressure vessel integrity  
Reactor vessel surveillance program  
Radiation embrittlement  
BWR  
Charpy testing  
Mechanical properties

# CONTENTS

---

<b>1 INTRODUCTION .....</b>	<b>1-1</b>
1.1 Implementation Requirements .....	1-2
<b>2 MATERIALS AND TEST SPECIMEN DESCRIPTION .....</b>	<b>2-1</b>
2.1 Dosimeters .....	2-1
2.2 Charpy V-Notch Specimens .....	2-1
2.2.1 Capsule Loading Inventory .....	2-1
2.2.2 Material Description and Properties .....	2-2
2.2.3 Chemical Composition .....	2-2
2.2.4 CVN Baseline Properties .....	2-5
2.3 Capsule Opening .....	2-7
<b>3 NEUTRON FLUENCE CALCULATION .....</b>	<b>3-1</b>
3.1 Description of the Reactor System .....	3-1
3.1.1 Reactor System Mechanical Design Inputs .....	3-1
3.1.2 Reactor System Material Compositions .....	3-3
3.1.3 Reactor Operating Data Inputs .....	3-3
3.1.3.1 Power History Data .....	3-3
3.1.3.2 Reactor State Point Data .....	3-4
3.1.3.3 Core Loading Pattern .....	3-6
3.2 Calculation Methodology .....	3-7
3.2.1 Description of the RAMA Fluence Methodology .....	3-7
3.2.2 The RAMA Geometry Model for Monticello .....	3-8
3.2.3 RAMA Calculation Parameters .....	3-11
3.2.4 RAMA Neutron Source Calculation .....	3-13
3.2.5 RAMA Fission Spectra .....	3-13
3.3 RAMA Nuclear Data Library .....	3-13
3.3.1 Nuclear Cross Sections .....	3-13

---

3.3.2 Activation Response Functions .....	3-15
3.4 Surveillance Capsule Activation Results .....	3-16
3.5 Surveillance Capsule Fluence Results .....	3-18
<b>4 CHARPY TEST DATA.....</b>	<b>4-1</b>
4.1 Charpy Test Procedure .....	4-1
4.2 Charpy Test Data .....	4-2
<b>5 CHARPY TEST RESULTS.....</b>	<b>5-1</b>
5.1 Analysis of Impact Test Results .....	5-1
5.2 Irradiated Versus Unirradiated CVN Properties .....	5-1
<b>6 REFERENCES .....</b>	<b>6-1</b>
<b>A APPENDIX A – DOSIMETER ANALYSIS.....</b>	<b>A-1</b>
A.1 Dosimeter Material Description.....	A-1
A.2 Dosimeter Cleaning and Mass Measurement.....	A-1
A.3 Radiometric Analysis .....	A-6

## LIST OF FIGURES

---

Figure 2-1 Monticello plate heat C2220 (LT) unirradiated Charpy energy plot .....	2-6
Figure 2-2 Photograph of Monticello 300° capsule .....	2-8
Figure 2-3 Photograph of Monticello 300° capsule Charpy Packet 5 .....	2-9
Figure 2-4 Photograph of Monticello 300° capsule Charpy Packet 4 .....	2-9
Figure 2-5 Photograph of Monticello 300° capsule Charpy Packet 10 .....	2-10
Figure 2-6 Photograph of Monticello 300° capsule Charpy Packet 9 .....	2-10
Figure 3-1 Planar view of Monticello at the core mid-plane elevation .....	3-2
Figure 3-2 Planar view of the Monticello RAMA quadrant model at the core mid-plane elevation .....	3-9
Figure 3-3 Axial view of the Monticello RAMA model .....	3-12
Figure 5-1 Irradiated plate C2220 (Monticello 300° capsule) Charpy energy plot .....	5-2
Figure 5-2 Irradiated plate C2220 (Monticello 300° capsule) lateral expansion plot .....	5-4
Figure A-1 P10-Cu dosimeter wire prior to cleaning .....	A-2
Figure A-2 P10-Cu dosimeter wire after cleaning .....	A-2
Figure A-3 P10-Cu dosimeter after cleaning and coiling .....	A-3
Figure A-4 P10-Fe dosimeter wire prior to cleaning .....	A-3
Figure A-5 P10-Fe dosimeter wire after cleaning .....	A-4
Figure A-6 P10-Fe dosimeter after cleaning and coiling .....	A-4
Figure A-7 P10-Ni dosimeter wire prior to cleaning .....	A-4
Figure A-8 P10-Ni dosimeter wire after cleaning .....	A-5
Figure A-9 P10-Ni dosimeter after cleaning and coiling .....	A-5

# LIST OF TABLES

Table 2-1 Monticello 300° surveillance capsule specimen inventory .....	2-2
Table 2-2 Results of the ICP analysis of two base metal samples (C2220) .....	2-3
Table 2-3 Analysis of the NIST traceable sample .....	2-4
Table 2-4 Best estimate chemistry of Monticello surveillance plate C2220 .....	2-4
Table 2-5 Unirradiated Charpy impact test data for surveillance plate C2220 (LT) .....	2-5
Table 2-6 Baseline CVN properties of plate heat C2220 (LT) .....	2-6
Table 3-1 Summary of material compositions by region for Monticello.....	3-4
Table 3-2 Number of state-point data files for each cycle in Monticello.....	3-5
Table 3-3 Summary of Monticello core loading pattern .....	3-6
Table 3-4 Energy boundaries for the RAMA neutron 47-group structure.....	3-14
Table 3-5 Row positions of response functions in tables 7001 and 7003.....	3-15
Table 3-6 Row positions of response functions in tables 7002 and 7004.....	3-16
Table 3-7 Comparison of specific activities for Monticello 300° surveillance capsule flux wires (c/m).....	3-17
Table 3-8 Average comparison of specific activities for Monticello 300° surveillance capsule flux wires by specimen packet .....	3-18
Table 3-9 Best estimate >1.0 MeV neutron fluence in Monticello 300° ISP capsule specimen packets .....	3-18
Table 4-1 Charpy V-notch impact test results for base metal specimens from the Monticello 300° surveillance capsule .....	4-2
Table 5-1 Effect of irradiation (E>1.0 MeV) on the notch toughness properties of plate heat C2220.....	5-6
Table 5-2 Comparison of actual versus predicted embrittlement.....	5-6
Table 5-3 Percent decrease in Upper Shelf Energy (USE).....	5-7
Table A-1 Wire dosimeter masses.....	A-6
Table A-2 GRSS specifications.....	A-7
Table A-3 Counting schedule for the dosimeter materials .....	A-8
Table A-4 Neutron-induced reactions of interest .....	A-8
Table A-5 Results of the radiometric analysis.....	A-9

# 1

## INTRODUCTION

---

Test coupons of reactor vessel ferritic beltline materials are irradiated in reactor surveillance capsules to facilitate evaluation of vessel fracture toughness in vessel integrity evaluations. The key values that characterize fracture toughness are the reference temperature of nil-ductility transition ( $RT_{NDT}$ ) and the upper shelf energy (USE). These are defined in 10CFR50 Appendix G [1] and in Appendix G of the ASME Boiler and Pressure Vessel Code, Section XI [2]. Appendix H of 10CFR50 [1] and ASTM E185-82 [3] establish the methods to be used for testing of surveillance capsule materials.

In the late 1990s the BWR Vessel and Internals Project (BWRVIP) initiated the BWRVIP Integrated Surveillance Program (ISP) [4], and the BWRVIP assumed responsibility for testing and evaluation of ISP capsules. The surveillance plate from the Monticello Nuclear Generating Plant (hereinafter, Monticello) was designated as an “ISP material” to be tested by the ISP according to an approved capsule withdrawal and test schedule. The other materials in the Monticello capsule – e.g., weld and HAZ specimens – are not used in the ISP and are not tested.

This report addresses the withdrawal and test of the Monticello 300° capsule. The capsule was irradiated for 23 cycles of operation; it was placed in the reactor’s 300° capsule holder prior to cycle 1 and was removed following cycle 23 for a total irradiation period of 28.2 effective full power years (EFPY). The capsule was removed in 2007 and testing and evaluation was completed in 2008. The surveillance capsule contained flux wires for neutron flux monitoring, Charpy V-notch impact test specimens, and tensile specimens. The capsule was shipped to MPM Research & Consulting for opening and testing of the surveillance plate specimens. Evaluation of the fluence environment was conducted by TransWare Enterprises, Inc. Final evaluation of the Charpy test data and irradiated material properties and compilation of this report were performed by ATI Consulting. The surveillance plate material was tested per ASTM E185-82, and the information and the associated evaluations provided in this report have been performed in accordance with the requirements of 10CFR50 Appendix B.

This report compares the irradiated material properties of surveillance plate heat C2220 to its baseline (e.g., unirradiated) properties. The observed embrittlement (as characterized by  $\Delta T_{30}$ ) is compared to that predicted by U.S. Nuclear Regulatory Commission (USNRC) Regulatory Guide 1.99, Rev. 2 [5]. Other BWRVIP ISP reports will integrate these shift results with previous Monticello surveillance capsule results for a broader characterization of embrittlement behavior.

## **1.1 Implementation Requirements**

The results documented in this report will be utilized by the BWRVIP ISP and by individual utilities to demonstrate compliance with 10CFR50, Appendix H, Reactor Vessel Material Surveillance Program Requirements. Therefore, the implementation requirements of 10CFR50, Appendix H govern and the implementation requirements of Nuclear Energy Institute (NEI) 03-08, Guideline for the Management of Materials Issues, are not applicable.

# 2

## MATERIALS AND TEST SPECIMEN DESCRIPTION

---

The General Electric-designed Monticello Nuclear Station (MNS) 300° surveillance capsule contained a total of two test specimen baskets. Each basket contained two Charpy packets and three tensile tubes. Within each Charpy packet were a total of 12 Charpy V-notch specimens and 3 high purity dosimetry wires. The 300° capsule is an original plant capsule and was irradiated in the plant since initial startup.

### 2.1 Dosimeters

The dosimetry wires were located along the ends of the Charpy specimens during irradiation. Further details on the exact wire locations during the irradiation are provided in the capsule opening discussion given in Section 2.3. A detailed discussion of the capsule dosimetry measurements is provided in Appendix A of this report.

### 2.2 Charpy V-Notch Specimens

The Charpy V-notch loading inventory, chemical compositions, material descriptions, and unirradiated (baseline) Charpy impact data, are summarized below.

#### 2.2.1 Capsule Loading Inventory

The specimen inventory of the 300° surveillance capsule is provided in Table 2-1. The goal was to extract and test only the base metal Charpy specimens. The weld and HAZ materials are not used in the BWRVIP ISP due to inadequate material traceability and baseline data and will not be tested or discussed further. The surveillance base metal specimens were machined from plate heat number C2220, and baseline data for this material is available.

As indicated in Table 2-1, there were a total of 4 Charpy packets in the capsule and each contained 3 dosimetry wires (one Fe wire, one Cu wire, and one Ni wire) and 12 Charpy specimens. There were no temperature monitors. Charpy packets 4 and 9 were found to contain all of the base metal test specimens. The packet loading did not correspond exactly with the plant documents, but the specimen identifications were positively made and verified with the FAB code markings.

**Table 2-1**  
**Monticello 300<sup>o</sup> surveillance capsule specimen inventory**

Monticello 300 <sup>o</sup> Surveillance Capsule Contents and Locations <sup>1</sup>							
Charpy Packet Number <sup>2</sup>	Number of Charpy Specimens			Number of Flux Wires			Relative Vertical Position
	Base	Weld	HAZ	Fe	Cu	Ni	
9	6	6	0	1	1	1	Highest in top basket
10	0	9	3	1	1	1	Lowest in top basket
4	8	4	0	1	1	1	Highest in bottom basket
5	0	4	8	1	1	1	Lowest in bottom basket

<sup>1</sup>The capsule included tensile specimens but the tensile specimens were not tested.

<sup>2</sup>The packet numbers in this table are organized by axial position in the capsule with packet 9 at the highest elevation and packet 5 at the lowest.

### 2.2.2 Material Description and Properties

The Monticello reactor pressure vessel was purchased from the Chicago Bridge and Iron Company (CB&I). The surveillance plate (heat C2220) Charpy specimens were machined with their longitudinal axis parallel to the plate rolling direction. The Charpy specimen notches were cut perpendicular to the plate surface and are designated longitudinal (LT) specimens [6]. The initial RT<sub>NDT</sub> of plate heat C2220 was previously reported to be 27°F [7].

### 2.2.3 Chemical Composition

New chemistry measurements on plate heat C2220 Charpy specimens were performed as part of this capsule test. Those measurements have been combined with previous chemistry measurements in order to determine a best estimate chemistry for surveillance plate C2220.

After the Charpy impact tests were conducted, chemical composition measurements were made on two base metal specimens to verify that the surveillance materials used to fabricate the specimens were actually cut from the correct vessel plate. The chemistry samples were machined from specimens "JDM" and "D14" using a clean end mill to ensure that no contamination of the sample occurred. The material was machined from the fracture surface ends of the specimen broken halves. Enough material was removed to provide a one gram sample for analysis.

Prior to analysis via Inductively Coupled Plasma-Mass Spectrometry (ICP-MS), the samples were cleaned by immersion in a bath of 100% ethyl alcohol to remove any surface contaminants. Duplicate samples of similar mass were taken for analysis for each specimen and the results averaged. The ICP-MS system used in this work is a quadrupole mass spectrometer manufactured by Perkin-Elmer and is designated as the Sciex ELAN 6000 system. It was calibrated using NIST traceable ICP standard solutions. The specimens taken for analysis were dissolved in an acid solution in preparation for introduction to the ICP-MS system. ICP-MS data were accumulated to show well-defined peaks for the elements of interest. Table 2-2 lists the elements of interest and the results obtained from the ICP-MS analysis. Review of the data confirms that the capsule base metal specimen results are in agreement with previously reported data for C2220.

**Table 2-2**  
**Results of the ICP analysis of two base metal samples (C2220)**

Element ID	Measured Concentration in Specimen "D14" (wt %)	Measured Concentration in Specimen "JDM" (wt %)
Cu	0.16	0.16
Fe <sup>(1)</sup>	97.14	97.15
Fe <sup>(2)</sup>	94.1	95.7
Mn	1.41	1.41
Mo	0.45	0.45
Ni	0.63	0.62
P	0.013	0.013
Si	0.19	0.20

<sup>1</sup> Concentration by difference (matrix element) for elements listed.

<sup>2</sup> Concentration by direct measurement.

In addition to the Charpy samples, the chemical analysis included a comparison with a NIST traceable steel sample, denoted as SRM 1262A (AISI 94B17). Table 2-3 shows the results of this study and comparison with accepted values. In general, there is good agreement. The measured values appear to scatter on either side of the expected values, with phosphorus showing a somewhat larger deviation than the other analytes.

Table 2-4 lists the previously available chemistry data for heat C2220, as well as the two new measurements. The measurements made on the two specimens from the 300° capsule were combined with existing measurements to determine a best estimate chemistry for the surveillance plate C2220. Reported measurements on different specimens were averaged in order to calculate the best estimate. In cases where multiple measurements had been reported for a single specimen, those measurements were first averaged to yield an average for that specimen, which was then considered with the other specimens. The bottom row of the table presents the final revised best estimate chemistry data.

**Table 2-3**  
**Analysis of the NIST traceable sample**

Element ID	Measured Concentration (wt %) for Sample STD	NIST Reported Concentration (wt %) for Sample STD	Percent Difference Between Reported and Measured Concentrations
Cu	0.51	0.51	0.0
Fe <sup>(1, 3)</sup>	97.28	96.7	0.6
Fe <sup>(2, 3)</sup>	95.4	95.3 <sup>(2, 3)</sup>	0.1
Mn	1.10	1.05	4.8
Mo	0.76	0.70	8.6
Ni	0.63	0.60	5.0
P	0.037	0.044	-15.9
Si	0.37	0.40	-7.5

<sup>1</sup> Concentration by difference (matrix element) for elements listed.

<sup>2</sup> Concentration by direct measurement.

<sup>3</sup> Fe concentration for this NIST sample is a recommended value (not certified).

**Table 2-4**  
**Best estimate chemistry of Monticello surveillance plate C2220**

Cu (Wt%)	Ni (Wt%)	P (Wt%)	S (Wt%)	Si (Wt%)	Mo (Wt%)	Mn (Wt%)	Specimen ID	Source
<b>0.16</b>	<b>0.68</b>	<b>0.010</b>	<b>0.020</b>	<b>0.23</b>	-	-	NUREG	Ref. 8
<b>0.17</b>	<b>0.58</b>	<b>0.010</b>	<b>0.014</b>	<b>0.22</b>	<b>0.45</b>	<b>1.31</b>	1-15	Ref. 9
0.166	0.659	0.005	0.010	0.315	0.431	1.41	C2220-2	Ref. 6
0.166	0.652	0.005	0.011	0.315	0.432	1.42	C2220-2	
0.165	0.662	0.004	0.011	0.315	0.442	1.42	C2220-2	
<b>0.166</b>	<b>0.658</b>	<b>0.005</b>	<b>0.011</b>	<b>0.315</b>	<b>0.435</b>	<b>1.42</b>	<b>Average C2220-2</b>	
0.165	0.651	0.011	0.011	0.299	0.430	1.41	JBL	Ref. 6
0.168	0.649	0.007	0.011	0.304	0.436	1.43	JBL	
0.165	0.653	0.009	0.010	0.318	0.437	1.41	JBL	
<b>0.166</b>	<b>0.651</b>	<b>0.009</b>	<b>0.011</b>	<b>0.307</b>	<b>0.434</b>	<b>1.42</b>	<b>Average JBL</b>	
<b>0.16</b>	<b>0.63</b>	<b>0.013</b>	-	<b>0.19</b>	<b>0.45</b>	<b>1.41</b>	D14	Table 2-2
<b>0.16</b>	<b>0.62</b>	<b>0.013</b>	-	<b>0.20</b>	<b>0.45</b>	<b>1.41</b>	JDM	Table 2-2
<b>0.16</b>	<b>0.64</b>	<b>0.010</b>	<b>0.014</b>	<b>0.24</b>	<b>0.44</b>	<b>1.39</b>	<b>Best Estimate Average</b>	

## 2.2.4 CVN Baseline Properties

As noted above, the Monticello surveillance plate Charpy specimens are longitudinal (LT) specimens. Table 2-5 shows the unirradiated (baseline) Charpy test data for the C2220 surveillance plate material, which was reported by NUREG-CR-6426 [8]. The baseline test data were fit to a hyperbolic tangent curve using the computer program CVGRAPH [10]; Figure 2-1 shows the fitted Charpy energy data. Table 2-6 summarizes the baseline (unirradiated) Charpy V-notch properties (index temperatures) of plate heat C2220. In this table and throughout this report,  $T_{30}$  is the 30 ft-lb (41 J) transition temperature;  $T_{50}$  is the 50 ft-lb (68 J) transition temperature;  $T_{35\text{mil}}$  is the 35 mil (0.89 mm) lateral expansion temperature; and USE is the average energy absorption at full shear fracture appearance.

**Table 2-5**  
Unirradiated Charpy impact test data for surveillance plate C2220 (LT)

Specimen ID	Temperature °F (°C)	CVN ft-lb (J)	Lateral Exp. mils (mm)	Percent Shear (%)
Z820	-50 (-45.6)	4.6 (6.2)	3.0 (0.1)	5
Z819	-25 (-31.7)	16.0 (21.7)	13.0 (0.3)	5
Z818	0 (-17.8)	22.0 (29.8)	18.0 (0.5)	10
Z817	25 (-3.9)	23.1 (31.3)	22.0 (0.6)	20
Z816	50 (10.0)	54.2 (73.5)	41.0 (1.0)	40
Z815	75 (23.9)	73.4 (99.5)	51.0 (1.3)	50
Z831	100 (37.8)	103.9 (140.9)	74.0 (1.9)	70
Z826	125 (51.7)	114.8 (155.6)	76.0 (1.9)	85
Z822	150 (65.6)	132.1 (179.1)	83.0 (2.1)	90
Z823	200 (93.3)	140.0 (189.8)	81.0 (2.1)	100
Z824	300 (148.9)	127.0 (172.2)	81.0 (2.1)	100
Z825	400 (204.4)	130.3 (176.7)	82.0 (2.1)	100

**Table 2-6**  
**Baseline CVN properties of plate heat C2220 (LT)**

Material Identity	Material	T <sub>30</sub> °F (°C)	T <sub>50</sub> °F (°C)	T <sub>35mil</sub> °F (°C)	Upper Shelf Energy (USE) ft-lb (J)
C2220 (LT)	Monticello Surveillance Plate	25.8 (-3.4)	48.6 (9.2)	40.7 (4.8)	132.4 (179.5)

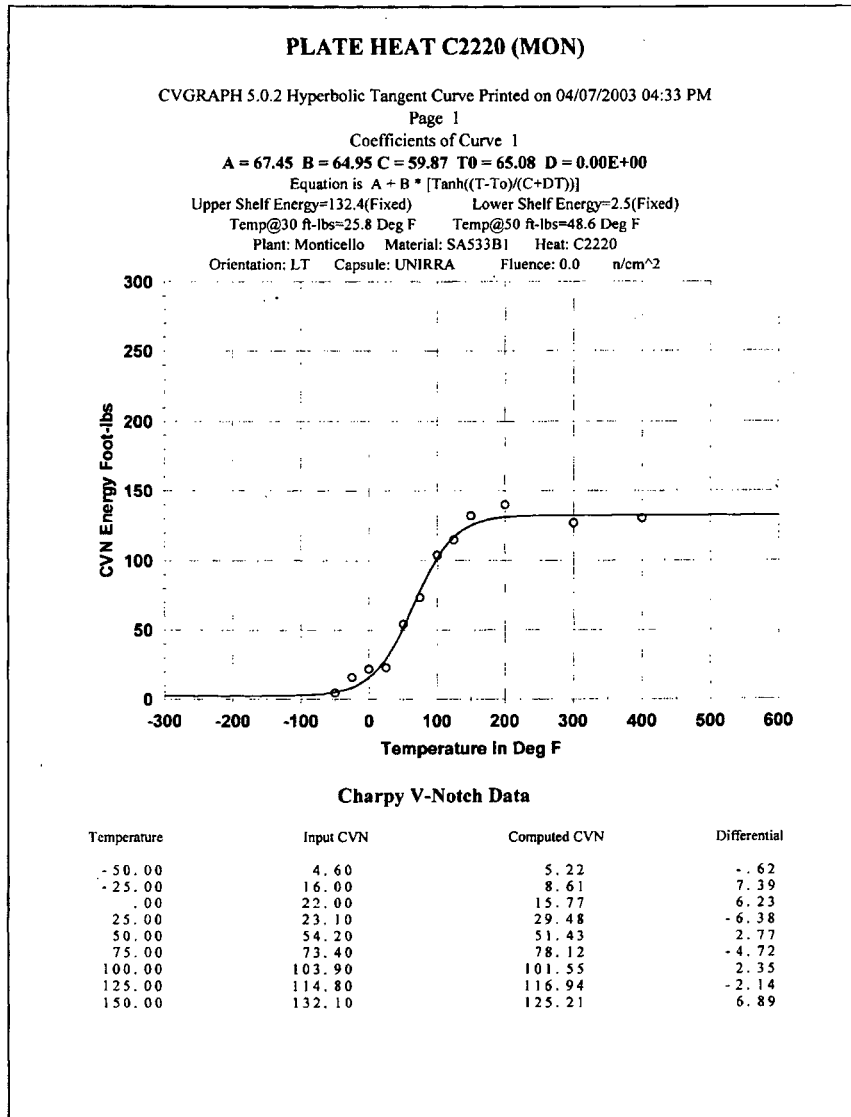


**Figure 2-1**  
**Monticello plate heat C2220 (LT) unirradiated Charpy energy plot**

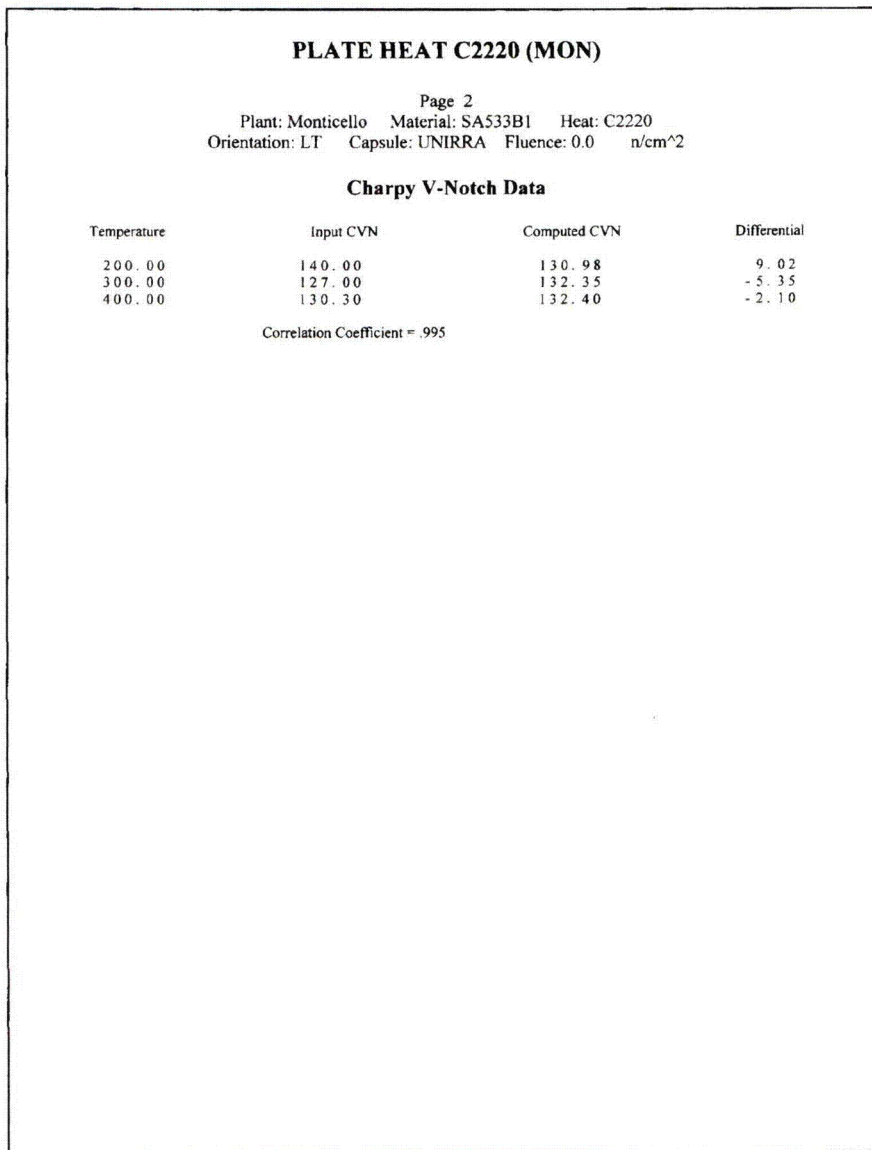


**Figure 2-1**  
Monticello plate heat C2220 (LT) unirradiated Charpy energy plot (continued)

### 2.3 Capsule Opening

The surveillance capsule was opened during October, 2007. As shown in Figure 2-2, the 300° capsule consisted of a double basket attached to the lead tube. The outside of the capsule had identification markings which could be clearly read. The capsule was marked with Reactor Code 19 and both baskets were marked with Basket Code 3. Each of the capsule baskets contained two Charpy packets and three tensile tubes.



**Figure 2-2**  
**Photograph of Monticello 300<sup>o</sup> capsule**

(Shows Double Basket and Positive Identification Markings. The Side which Faced the Pressure Vessel in the Plant is Facing up in this Photograph)

Referring to Figure 2-2, the lead tube is positioned on the underside of the baskets in the photograph. Therefore, the surface that is up in the photograph was facing the vessel during irradiation. The hook at the top of the photograph is the vessel attachment hook and it is on the bottom of the capsule when it is installed in the plant. The Charpy Packet end tabs are on the right side in Figure 2-2. Moving up from the bottom of the capsule, the first item in the capsule is Charpy Packet 5, then there are 3 tensile tubes, and finally Charpy Packet 4 is located at the top side of the lower basket. Continuing vertically upward, the upper basket contains Charpy Packet 10, followed by 3 tensile tubes, and Charpy Packet 9 is located at the top side of the upper basket. Photographs of the Charpy packets in the axial position order discussed are shown in Figures 2-3 through 2-6. These photographs show the arrangement of the Charpy specimens inside of each packet and also show the Charpy Packet binary code marking on the end tabs.

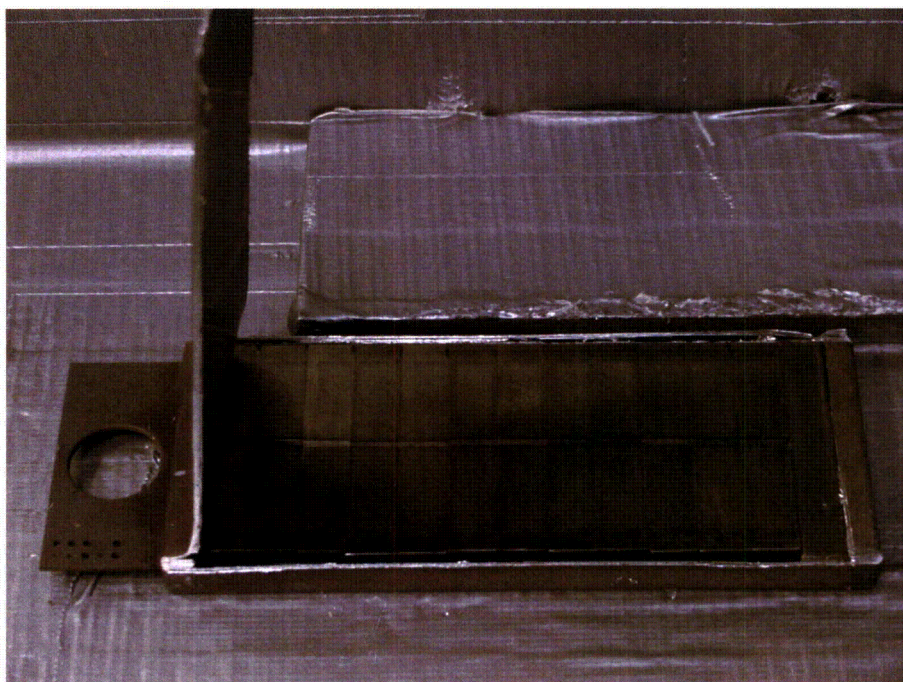


Figure 2-3  
Photograph of Monticello 300<sup>o</sup> capsule Charpy Packet 5

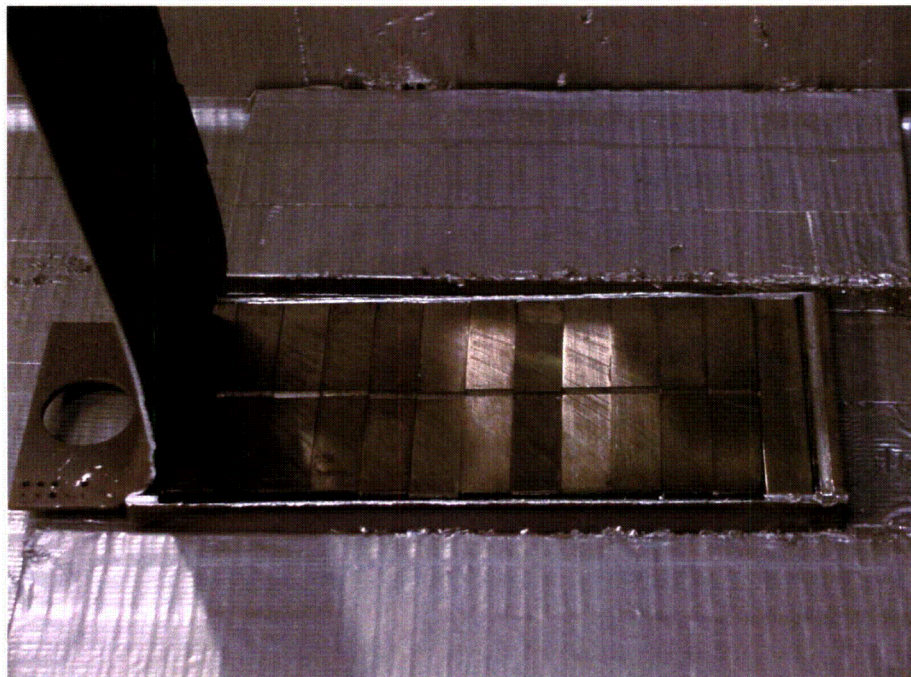
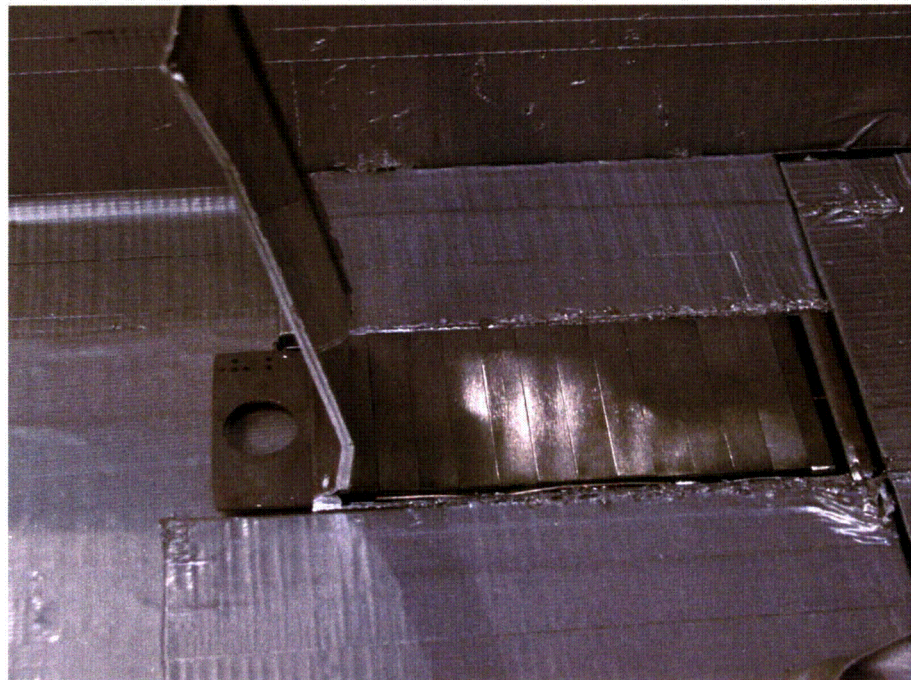


Figure 2-4  
Photograph of Monticello 300<sup>o</sup> capsule Charpy Packet 4



**Figure 2-5**  
**Photograph of Monticello 300° capsule Charpy Packet 10**



**Figure 2-6**  
**Photograph of Monticello 300° capsule Charpy Packet 9**

Attention was paid to the location of the Charpy specimens and the dosimetry wire locations during disassembly of the Charpy packets. Each packet was found to contain one Fe, one Cu, and one Ni dosimetry wire. The wires and Charpy specimens were placed in individually marked containers for positive identification throughout the work. The wires were located along the ends of the Charpy specimens on one side of the Charpy packet. Therefore, the wires were irradiated in a horizontal position in the reactor. For Charpy Packets 4 and 5, the 3 wires were located on the bottom side of the packets. For Charpy Packets 9 and 10, the wires were located on the top side of the packets.

The position of the Charpy specimens along the length of the packets was also recorded during disassembly. The plant documentation indicates that Charpy Packets 5 and 10 should contain only 4 weld and 8 HAZ material Charpy specimens each, and this was confirmed by the test specimen IDs for Packet 5. However, Packet 10 contained 9 weld and 3 HAZ specimens. The plant records indicated that Charpy Packets 4 and 9 should contain 8 base metal and 4 weld metal Charpy specimens. This was found to be true for Packet 4. However, Packet 9 was found to contain 6 base metal Charpy and 6 weld metal Charpy specimens. Therefore, a total of 14 base metal Charpy specimens were recovered for impact testing.

# 3

## NEUTRON FLUENCE CALCULATION

---

The modeling and analysis guidelines provided in Regulatory Guide 1.190 [11] were used to determine the surveillance capsule accumulated irradiation and capsule specimen neutron fluence of the Monticello 300° ISP capsule flux wires. The fluence and activation values were calculated using the RAMA Fluence Methodology [12] (hereinafter referred to as “RAMA”). The specific activities predicted by RAMA are compared to the activity measurements from the capsule dosimetry.

RAMA was developed for the Electric Power Research Institute, Inc. (EPRI) and the Boiling Water Reactor Vessel and Internals Project (BWRVIP) for the purpose of calculating neutron fluence in Boiling Water Reactor (BWR) components. RAMA has been approved by the U.S. Nuclear Regulatory Commission [13, 14] for application in accordance with U.S. Regulatory Guide 1.190. Benchmark testing has been performed for several surveillance capsule and RPV fluence evaluations using RAMA. Results of these benchmark efforts show that RAMA accurately predicts fluence in the RPV and surveillance capsule components of BWRs [15].

### 3.1 Description of the Reactor System

This section describes the Monticello model used in the surveillance capsule activation and fluence evaluation. The fluence model is based on plant-specific design inputs including component mechanical designs, material compositions, and reactor operating history. Plant-specific mechanical design drawings and structural material data were provided by Monticello and were used to build the Monticello RAMA geometry model. Core simulator data representing the historical operating conditions of the reactor was provided for cycles 10 through 23. Core simulator data was not available for cycles 1 through 9. Data for these cycles was approximated using information from cycle summary reports and nodal software combined with detailed operating data from cycles of comparable core design and energy production.

#### 3.1.1 Reactor System Mechanical Design Inputs

Monticello is a General Electric BWR/3 class reactor with a core loading of 484 fuel assemblies. The Monticello reactor is modeled with RAMA. RAMA employs a three-dimensional combinatorial geometry modeling technique to describe the reactor geometry for the neutron transport calculations. Detailed plant mechanical design information is used in order to build an accurate three-dimensional computer model of the reactor system.

Figure 3-1 illustrates the basic planar geometry configuration of the reactor at the axial elevation corresponding to the core mid-plane. All radial regions comprising the fluence model are illustrated. Beginning at the center of the reactor and projecting outward, the regions include: the core region, including control rod locations and fuel assembly locations (fuel locations are shown only for the 0 to 90 degree quadrant); core reflector region (bypass water); central shroud wall; downcomer water region including the jet pumps; reactor pressure vessel (RPV) wall; mirror insulation; biological shield (concrete wall); and cavity regions between the RPV and biological shield. Also shown are the azimuthal positions of the surveillance capsules in the downcomer region at 30, 120, and 300 degrees and the jet pump assemblies at 30, 60, 90, 120, 150, 210, 240, 270, 300 and 330 degrees.

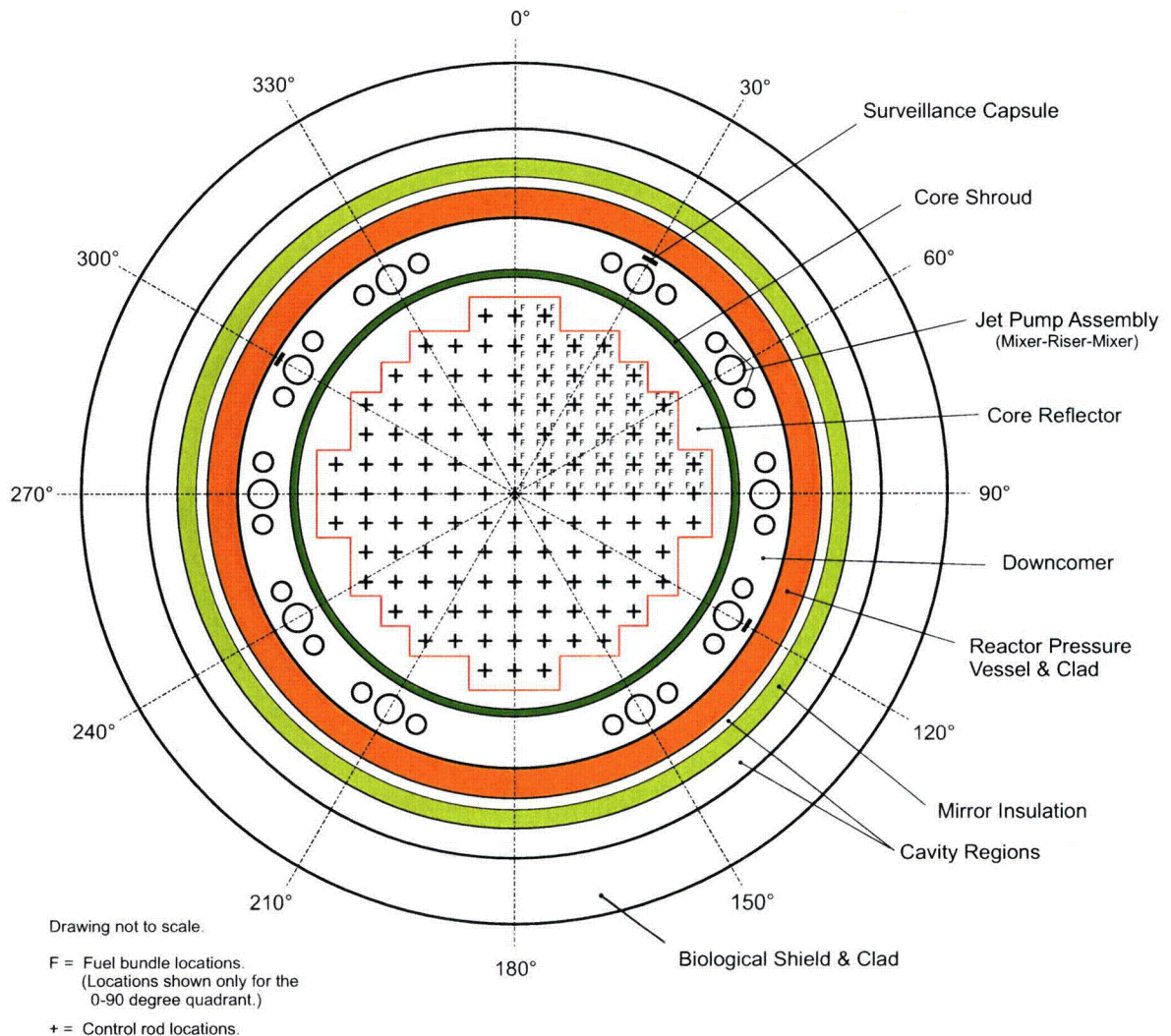


**Figure 3-1**  
Planar view of Monticello at the core mid-plane elevation

### **3.1.2 Reactor System Material Compositions**

Each region of the reactor is comprised of materials that include reactor fuel, steel, water, insulation, concrete, and air. Accurate material information is essential for the fluence evaluation as the material compositions determine the scattering and absorption of neutrons throughout the reactor system and, thus, affect the determination of neutron fluence in the reactor components.

Table 3-1 provides a summary of the material compositions in the various components and regions of the Monticello reactor. The attributes for the steel, insulation, and air compositions (i.e. material densities and isotopic concentrations) are assumed to remain constant for the operating life of the reactor. The coolant water densities in the ex-core regions can vary with reactor heat balance through and between operating cycles, but are generally represented as constant values over a cycle at the rated hot operating conditions for the cycle. The attributes of the fuel compositions in the reactor core region change continuously during an operating cycle due to changes in power level, fuel burnup, control rod movements, and changing moderator density levels (voids). Because of the dynamics of the fuel attributes with reactor operation, one to several data sets are used to describe the operating states of the reactor core throughout each operating cycle. The number of data sets used in this analysis is presented in Section 3.1.3.2.

### **3.1.3 Reactor Operating Data Inputs**

An accurate evaluation of fluence in the reactor requires an accurate accounting of the reactor operating history. The primary reactor operating parameters that affect neutron fluence evaluations for BWR's include the reactor power level, core power distribution, core void fraction distribution (or equivalently, water density distribution), and fuel material distribution. These items are described in the following subsections.

#### **3.1.3.1 Power History Data**

The reactor power history used in the Monticello surveillance capsule activation and fluence evaluation was based on daily power history edits provided by Monticello for operating cycles 1 through 23. The daily power values represent step changes in power on a daily basis and are assumed to be representative of the power over the entire day. The power history data accounts for the reactor shutdown periods. Table 3-2 provides the accumulated effective full power years of power generation at the end of each cycle in this fluence evaluation.

The rated thermal power output of the Monticello reactor for operating cycles 1 through the first half of cycle 19 (19a) is 1670 MWt. A power uprate was achieved in the middle of cycle 19 (19b), raising the thermal power to 1775 MWt for the remainder of the irradiation period.

**Table 3-1**  
**Summary of material compositions by region for Monticello**

Region	Material Composition
Control Rods and Guide Tubes	Stainless Steel and B <sub>4</sub> C
Core Support Plate	Stainless Steel
Fuel Support Piece	Stainless Steel and B <sub>4</sub> C
Fuel Bundle Lower Tie Plate	Stainless Steel, Zircaloy, Inconel
Reactor Core	<sup>235</sup> U, <sup>238</sup> U, <sup>239</sup> Pu, <sup>240</sup> Pu, <sup>241</sup> Pu, <sup>242</sup> Pu, O <sub>fuel</sub> , Zircaloy, Water
Core Reflector	Water
Fuel Bundle Upper Tie Plate	Stainless Steel, Zircaloy, Inconel
Top Guide	Stainless Steel
Core Spray Sparger Pipes	Stainless Steel
Core Spray Sparger Flow Areas	Water
Shroud	Stainless Steel
Downcomer Region	Water
Jet Pump Riser and Mixer Flow Areas	Water
Jet Pump Riser and Mixer Metal	Stainless Steel
Surveillance Capsule Specimens	Carbon Steel
Reactor Pressure Vessel Clad	Stainless Steel
Reactor Pressure Vessel Wall	Carbon Steel
Cavity Regions	Air
Insulation	Aluminum, Stainless Steel
Biological Shield Clad	Carbon Steel
Biological Shield Wall	Reinforced Concrete

### 3.1.3.2 Reactor State Point Data

Reactor operating data in the form of state-point data files was used in the Monticello surveillance capsule activation and fluence evaluation. The state-point files provide a best-available representation of the operating conditions of the reactor core over the operating life of the reactor. The data files include three-dimensional data arrays that describe the fuel materials, moderator materials, and relative power distribution in the core region.

A separate neutron transport calculation was performed for each of the available state points. The calculated neutron flux for each state point was combined with the appropriate power history

data described in Section 3.1.3.1 in order to predict the neutron fluence in the surveillance capsules.

A total of 213 state-point data files were used to represent the first 23 operating cycles of Monticello. Table 3-2 shows the number of state points used for each cycle in this fluence evaluation. Detailed core simulator data with nodal and pin power distributions was used for cycles 10 through 23. Limited core simulator data with nodal average power distributions was used for cycles 6 through 9. No core simulator data was available for cycles 1 through 5, so state-point data for these cycles was approximated using information from cycle summary reports combined with detailed operating data from later cycles of comparable core design and energy production.

**Table 3-2**  
**Number of state-point data files for each cycle in Monticello**

Cycle Number	Number of State Point Data Files	Rated Thermal Power <sup>(a)</sup> MWt	Accumulated Effective Full Power Years (EFPY)
1	3	1670	1.2
2	3	1670	1.9
3	3	1670	2.4
4	3	1670	2.8
5	3	1670	4.4
6	8	1670	5.2
7	10	1670	6.4
8	7	1670	7.2
9	10	1670	8.2
10	7	1670	9.2
11	12	1670	10.3
12	8	1670	11.5
13	12	1670	12.9
14	9	1670	14.2
15	12	1670	15.8
16	10	1670	17.2
17	11	1670	18.6
18	9	1670	20.1
19a	2	1670	21.7
19b	6	1775	
20	13	1775	23.2
21	11	1775	24.5
22	18	1775	26.3
23	23	1775	28.2

a) The rated thermal power level is listed for each cycle. However, actual power levels for the individual state points were used in calculations for cycles 1 through 23.

### 3.1.3.3 Core Loading Pattern

It is common in BWRs that more than one fuel assembly design will be loaded in the reactor core in any given operating cycle. For fluence evaluations, it is important to account for the fuel assembly designs that are loaded in the core in order to accurately represent the neutron source distribution at the core boundaries (i.e., peripheral fuel locations, the top fuel nodes, and the bottom fuel nodes).

Ten different fuel assembly designs were loaded in the reactor during cycles 1 through 23. Table 3-3 provides a summary of the fuel designs loaded in the reactor core for these operating cycles. The cycle core loading patterns provided by Monticello were used to identify the fuel assembly designs in each cycle and their location in the core loading pattern. For each cycle, appropriate fuel assembly models were used to build the reactor core region of the RAMA fluence model for Monticello.

**Table 3-3**  
**Summary of Monticello core loading pattern**

Cycle	7x7 Fuel Assembly Designs	8x8 Fuel Assembly Designs					9x9 Fuel Assembly Designs		10x10 Fuel Assembly Designs	
	GE3	GE4	GE6/7	GE8	GE9	GE10	SPC 9x9	GE11	GE12	GE14
1	484									
2	484									
3	368	116								
4	288	196								
5	20	464								
6		484								
7		372	112							
8		272	212							
9		184	300							
10		84	400							
11		92	392							
12		44	440							
13			364	120						
14			236	120	128					
15			100	120	128	136				
16				92	128	264				

**Table 3-3 (continued)**  
**Summary of Monticello core loading pattern**

Cycle	7x7 Fuel Assembly Designs	8x8 Fuel Assembly Designs					9x9 Fuel Assembly Designs		10x10 Fuel Assembly Designs	
	GE3	GE4	GE6/7	GE8	GE9	GE10	SPC 9x9	GE11	GE12	GE14
17					108	368	8			
18						332	8	140	4	
19						204	8	268	4	
20						68		412	4	
21								376	4	104
22								244		240
23								92		392

Note: The dominant peripheral fuel design represented in the RAMA model is highlighted in yellow for each cycle.

## 3.2 Calculation Methodology

The Monticello capsule evaluation was performed using the RAMA Fluence Methodology software package [12]. RAMA and the application of RAMA to the Monticello reactor are described in this section.

### 3.2.1 Description of the RAMA Fluence Methodology

RAMA is a system of codes that is used to perform fluence evaluations in light water reactor components. RAMA includes a transport code, model builder codes, a fluence calculator code, an uncertainty methodology, and a nuclear data library. The transport code, fluence calculator, and nuclear data library are the primary software components for calculating the neutron flux and fluence. The transport code uses a deterministic, three-dimensional, multigroup nuclear particle transport theory to perform the neutron flux calculations. The transport code couples the nuclear transport method with a general geometry modeling capability to provide a flexible and accurate tool for calculating fluxes in light water reactors. The fluence calculator uses reactor operating history information with isotopic production and decay data to estimate activation and fluence in the reactor components over the operating life of the reactor. The nuclear data library contains nuclear cross-section data and response functions that are needed in the flux, fluence, and reaction rate calculations. The cross sections and response functions are based on the BUGLE-96 nuclear data library [16]. RAMA and procedures for its use are described in the following reports: Theory Manual [17] and Procedures Manual [18].

The primary inputs for RAMA are mechanical design parameters and reactor operating history data. The mechanical design inputs are obtained from reactor design drawings (or vendor drawings) of the plant. The reactor operating history data is obtained from reactor core simulation calculations, system heat balance calculations, and daily operating logs that describe the operating conditions of the reactor.

The primary outputs from RAMA calculations are neutron flux, neutron fluence, and uncertainty determinations. The RAMA transport code calculates the neutron flux distributions that are used in the determination of neutron fluence. Several transport calculations are typically performed over the operating life of the reactor in order to calculate neutron flux distributions that accurately characterize the operating history of the reactor. The post-processing code (RAFTER) is then used to calculate component fluence and nuclide activations using the neutron flux solutions from the transport calculations and daily operating history data for the plant.

### **3.2.2 The RAMA Geometry Model for Monticello**

RAMA uses a flexible three-dimensional modeling technique to describe the reactor geometry. The geometry modeling technique is based on the Cartesian coordinate system in which the (x,y) coordinates describe an axial plane of the reactor system and the z-axis describes elevations of the reactor system.

Figure 3-2 illustrates the planar configuration of the Monticello model in azimuthal quadrant mirror symmetry at an axial elevation near the core mid-plane of the reactor pressure vessel. In the radial dimension the model extends from the center of the RPV to the outside surface of the biological shield (382.75 cm). Nine radial regions are defined in the Monticello model: the core region (comprised of interior and peripheral fuel assemblies), core reflector, shroud, downcomer region, pressure vessel, mirror insulation, biological shield, and inner and outer cavity regions. The pressure vessel has cladding on the wall inner surface. The biological shield has cladding on the inner and outer surfaces. The downcomer region includes representations for the jet pumps and surveillance capsules.

Figure 3-2 shows that the reactor core region is modeled with rectangular geometry to preserve the shape of the core region. The core region model is characterized in two layers: the interior fuel assemblies and the peripheral fuel assemblies. The peripheral fuel assemblies are the primary contributors to the neutron source in the fluence calculation and are modeled to preserve the pin-wise source contribution at the core-core reflector interface.

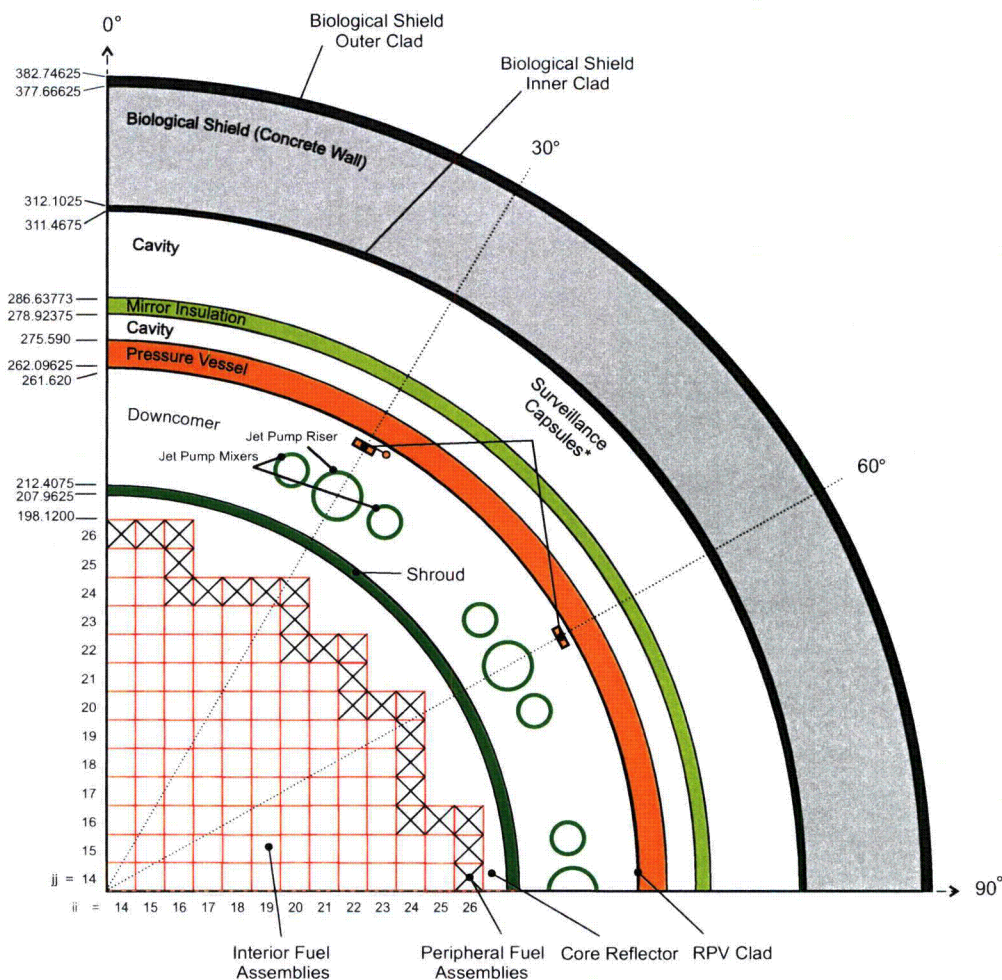
Each of the components and regions that extend outward from the core region are modeled in their correct geometrical form. The core shroud, downcomer, RPV wall, mirror insulation, biological shield wall, and cavity regions are modeled as cylindrical parts. The shapes of other significant reactor components are appropriately represented in the model.

The surveillance capsule, which is rectangular in design, is modeled as an arc element in the geometry and is correctly positioned behind the jet pump riser pipe at a radial position near the inner surface of the RPV wall. This model is an acceptable approximation since the capsule is a

sufficient distance from the core center that the arc element closely approximates the shape of a rectangular element. Downcomer water surrounds the capsule on all sides.

The jet pump assembly design is modeled using cylindrical pipe elements for the jet pump riser and mixer pipes. The riser pipe is correctly situated on a curvilinear path between the centers of the mixer pipes.

As shown in Figure 3-2, Monticello geometry is modeled in quadrant mirror symmetry, both in the core region and in the ex-core geometry. The ex-core symmetry results from the presence of ten jet pump assemblies that are located in quadrant-symmetric locations. In the azimuthal dimension, the RAMA model spans from 0 to 90 degrees where the 0 degree azimuth corresponds to the reactor vessel 0 degree azimuth.



Note: Dimensions given in centimeters. Drawing not to scale.  
 \*Capsule at 60° represents capsules at 120° and 300° locations. The 30° capsule's flux wire holder is included in the model.

**Figure 3-2**  
**Planar view of the Monticello RAMA quadrant model at the core mid-plane elevation**

The jet pumps are shown, as modeled, at azimuths 30, 60 and 90 degrees in the downcomer region. When symmetry is applied to the model, the 30 degree location represents the jet pump assemblies that are positioned azimuthally at 30, 150, 210, and 330 degrees; the 60 degree location represents the jet pump assemblies at 60, 120, 240, and 300 degrees; and the 90 degree location represents the jet pump assemblies at 90 and 270 degrees.

The surveillance capsules are shown as modeled at azimuth 30 and 60 degrees. When symmetry is applied to the model, the 60 degree location represents each of the surveillance capsules installed at 120 and 300 degrees.

Figure 3-3 provides an illustration of the axial configuration of the Monticello RAMA model for four significant components: a fuel column, the core shroud, the downcomer region, and the reactor pressure vessel. Also shown in the figure is the relative axial positioning of the jet pumps, surveillance capsules, top guide, RPV circumferential welds, and core spray sparger pipes in the reactor model. The 30° capsule is taller than the 300° capsule, and is accurately represented as such in the model. Each jet pump in Monticello is supported by two riser braces that connect the jet pump riser pipe to the RPV wall. The lower riser brace is explicitly modeled since it is directly between the capsule and the core and has a shielding effect on the capsule. The upper riser brace is physically smaller and is above the capsules, so it was not modeled since it will not have a noticeable effect on the capsule fluence.

The axial planes are divided into several groups representing particular component regions of the model as follows: the core region, the top guide, the shroud head flange, the core spray spargers, the fuel support piece, core support plate, and core inlet region. Sub-planar meshing is used in the model, as needed, to properly represent the positioning of reactor components, such as the surveillance capsules and jet pump rams head. Fluence is calculated at the elevations for the surveillance capsules depicted in the figure. The Monticello fluence model consists of over 100,000 mesh regions. In the axial direction, the Monticello fluence model spans from below the jet pump riser inlet to above the core shroud head flange for a total of 640.08 cm (21 feet) in height.

There are several key features of the RAMA code system that allow the reactor design to be accurately represented for capsule fluence evaluations. Following is a list of some of the key features of the model.

- Rectangular and cylindrical bodies are mixed in the model in order to provide an accurate geometrical representation of the components and regions in the reactor.
- The core geometry is modeled using rectangular bodies to represent the fuel assemblies in the reactor core region.
- Cylindrical bodies are used to represent the components and regions that extend outward from the core region.
- A combination of rectangular and cylindrical bodies is used to describe the transition parts that are required to interface the rectangular core region to the cylindrical outer core regions.

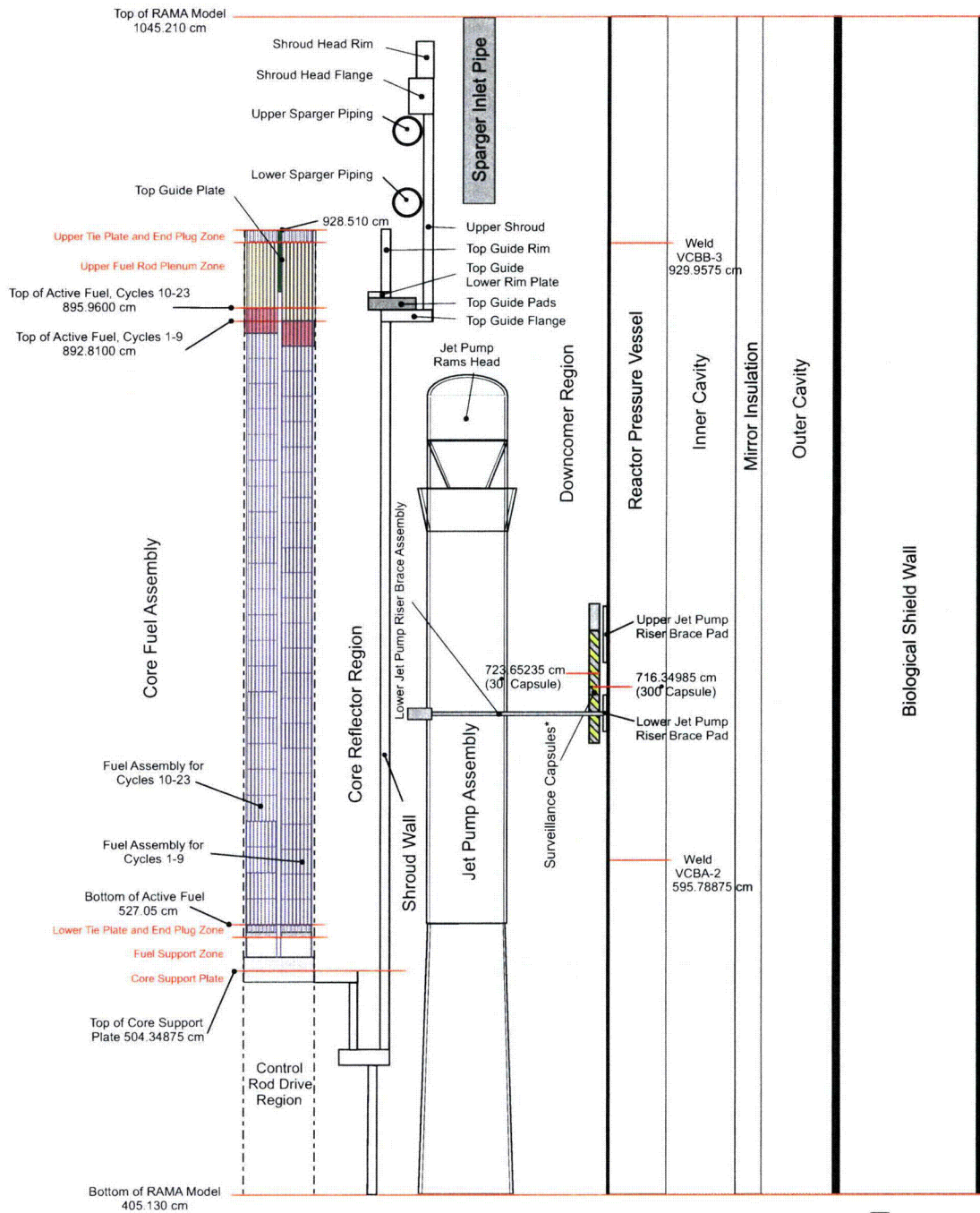
- The top guide is appropriately modeled by including a representation of the vertical fuel assembly parts and top guide plates. The upper fuel assembly parts that extend into the top guide region are modeled in three axial segments: the fuel rod plenum, fuel rod upper end plugs, and fuel assembly upper tie plate.
- The jet pump assembly model includes representations of the riser, mixer, and diffuser pipes; nozzles; rams head; and riser brace yoke, leaves, and pads.
- The surveillance capsules are represented in the downcomer region at the correct azimuth, at an axial elevation corresponding to the core mid-plane elevation, and radially near the inner surface of the pressure vessel wall.
- The core spray spargers are appropriately represented as toruses in the model. The sparger pipes and nozzles reside inside the upper shroud wall above the top guide. The sparger model includes a representation of reactor coolant inside the pipes.
- The fuel support piece, core support plate, and core inlet regions appropriately include a representation of the cruciform control rod below the core region. The lower fuel assembly parts include representations for the fuel rod lower end plugs, lower tie plate, and nose piece.

### **3.2.3 RAMA Calculation Parameters**

The RAMA transport code uses a three-dimensional deterministic transport method to calculate neutron flux distributions in reactor problems. The transport method is based on a numerical integration technique that uses ray-tracing to form the integration paths through the problem geometry. The integration paths for the rays are determined using four parameters. The distance between parallel rays in the planar dimension is specified as 0.80 cm. The distance between parallel rays in the axial dimension is specified as 4.50 cm. The depth that a ray penetrates a reflective boundary is specified as 10 mean free paths. The angular quadrature for determining ray trajectories is specified as S8, which provides an acceptable compromise between computational accuracy and performance.

The RAMA transport calculation also uses information from the RAMA nuclear data library to determine the scope of the flux calculation. This information includes the Legendre expansion of the scattering cross sections that is used in the treatment of anisotropy of the problem. By default, the RAMA transport calculation uses the maximum order of expansion that is available for each nuclide in the RAMA nuclear data library (i.e. through  $P_5$  scattering for actinide and zirconium nuclides and through  $P_7$  scattering for all other nuclides in the model).

The neutron flux is calculated using an iterative technique to obtain a converged solution for the problem. The convergence criterion used in the evaluation is 0.01, which provides an asymptotic solution.



\* The 30° and 300° capsules are shown. The 30° capsule is designated by the [blue square] color and the 300° capsule is designated by the [yellow square] color.

Drawing not to scale.

**Figure 3-3**  
**Axial view of the Monticello RAMA model**

### **3.2.4 RAMA Neutron Source Calculation**

The neutron source for the RAMA transport calculation is calculated using the input relative power density factors for the different fuel regions and data from the RAMA nuclear data library.

The core neutron source is determined using the cycle-specific three-dimensional burnup distributions. The radial power gradient in the peripheral fuel assemblies is modeled to account for the pin-wise source distributions in the peripheral and inside corner fuel assemblies.

When pin-wise power data is not available, the nodal average power is used for each pin location, representing a flat power distribution over the bundle. This approach yields a more conservative power shape in the absence of more detailed information.

### **3.2.5 RAMA Fission Spectra**

RAMA calculates a weighted fission spectrum, based on the relative contributions of the fuel isotopes, that is used in the transport calculation. The fission spectra for <sup>235</sup>U, <sup>238</sup>U, <sup>239</sup>Pu, <sup>240</sup>Pu, <sup>241</sup>Pu, and <sup>242</sup>Pu that are used in the RAMA transport calculations were taken directly from the latest release of the BUGLE-96 data library.

## **3.3 RAMA Nuclear Data Library**

The nuclear cross section library is an essential element in neutron fluence evaluations. The accuracy of the cross section data is one of the primary factors that affect the accuracy of the neutron fluence prediction in reactor components. The RAMA nuclear data library is based upon the BUGLE-96 library [16] which has been developed exclusively from ENDF/B-VI nuclear data by Oak Ridge National Laboratory.

### **3.3.1 Nuclear Cross Sections**

The RAMA nuclear data library consists of 47 neutron energy groups that span an energy range of 0.1 eV to 17.332 MeV. The group structure is especially well-suited to applications requiring accurate determination of neutron flux with energy >1.0 MeV. This is of primary importance in the evaluation of irradiation damage to reactor components. The RAMA nuclear data library also includes energy group upscattering in the lower (thermal) energy range of <5.04 eV. This significantly improves the prediction of thermal flux. Table 3-4 shows the group structure for the 47 neutron groups in the RAMA nuclear data library. The RAMA nuclear data library contains an extensive set of nuclide cross sections that are pre-shielded and spectrally collapsed using light water reactor flux spectra. The library incorporates improved resonance treatments for steel nuclides that are based on ENDF-B/VI. The resonance treatments are of particular importance in reactor system component fluence evaluations. Except for oxygen in the reactor cavity regions, surveillance capsule evaluations use appropriately pre-shielded and spectrally collapsed cross section data.

The RAMA nuclear data library has been especially developed for the solution of ex-core neutron transport calculations that must account for anisotropic scattering effects. Lighter

nuclides contain scattering data for up to P7 Legendre scattering expansion, while the heavier nuclides contain data for up to P5 scattering.

**Table 3-4**  
**Energy boundaries for the RAMA neutron 47-group structure**

Energy Group	Upper Energy (eV)	Energy Group	Upper Energy (eV)
1	1.7332E+07	25	2.9721E+05
2	1.4191E+07	26	1.8316E+05
3	1.2214E+07	27	1.1109E+05
4	1.0000E+07	28	6.7379E+04
5	8.6071E+06	29	4.0868E+04
6	7.4082E+06	30	3.1828E+04
7	6.0653E+06	31	2.6058E+04
8	4.9659E+06	32	2.4176E+04
9	3.6788E+06	33	2.1875E+04
10	3.0119E+06	34	1.5034E+04
11	2.7253E+06	35	7.1017E+03
12	2.4660E+06	36	3.3546E+03
13	2.3653E+06	37	1.5846E+03
14	2.3457E+06	38	4.5400E+02
15	2.2313E+06	39	2.1445E+02
16	1.9205E+06	40	1.0130E+02
17	1.6530E+06	41	3.7266E+01
18	1.3534E+06	42	1.0677E+01
19	1.0026E+06	43	5.0435E+00
20	8.2085E+05	44	1.8554E+00
21	7.4274E+05	45	8.7643E-01
22	6.0810E+05	46	4.1399E-01
23	4.9787E+05	47	1.0000E-01
24	3.6883E+05	-	1.0000E-05

### 3.3.2 Activation Response Functions

Response functions are used to calculate nuclear reactions and other integral parameters (e.g., integrated fluxes over various energy ranges) of interest in ex-core calculations. Tables 3-5 and 3-6 list the activation response functions included in the RAMA nuclear data library.

**Table 3-5**  
Row positions of response functions in tables 7001 and 7003

Row	Response	Row	Response
1	Group upper energy (MeV)	29	I-127 (n,2n) I-126
2	U-235 fission spectrum (chi)	30	Sc-45 (n, $\gamma$ ) Sc-46
3	Li-6 (n,x) He-4	31	Na-23 (n, $\gamma$ ) Na-24
4	B-10 (n, $\alpha$ ) Li-7	32	Fe-58 (n, $\gamma$ ) Fe-59
5	Th-232 (n,fission)	33	Co-59 (n, $\gamma$ ) Co-60
6	U-235 (n,fission)	34	Cu-63 (n, $\gamma$ ) Cu-64
7	U-238 (n,fission)	35	In-115 (n, $\gamma$ ) In-116
8	Np-237 (n,fission)	36	Au-197 (n, $\gamma$ ) Au-198
9	Pu-239 (n,fission)	37	Th-232 (n, $\gamma$ ) Th-233
10	Al-27 (n,p) Mg-27	38	U-238 (n, $\gamma$ ) U-239
11	Al-27 (n, $\alpha$ ) Na-24	39	$\sqrt{E_{Mid}} (MeV^{1/2})$
12	S-32 (n,p) P-32	40	Total neutron flux
13	Ti-46 (n,p) Sc-46	41	U-234 (n,fission)
14	Ti-47 (n,p) Sc-47	42	U-236 (n,fission)
15	Ti-47 (n,n'p) Sc-46	43	Pu-240 (n,fission)
16	Ti-48 (n,p) Sc-48	44	Pu-241 (n,fission)
17	Ti-48 (n,n'p) Sc-47	45	Pu-242 (n,fission)
18	Mn-55 (n,2n) Mn-54	46	Rh-103 (n,n') Rh-103m
19	Fe-54 (n,p) Mn-54	47	Si displacement kerma (eV·b)
20	Fe-56 (n,p) Mn-56	48	U-238 fission spectrum (chi)
21	Co-59 (n,2n) Co-58	49	Pu-239 fission spectrum (chi)
22	Co-59 (n, $\alpha$ ) Mn-56	50	E > 1.0 MeV neutron flux
23	Ni-58 (n,p) Co-58	51	E > 0.1 MeV neutron flux
24	Ni-58 (n,2n) Ni-57	52	E < 0.414 eV neutron flux
25	Ni-60 (n,p) Co-60	53	Average energy (MeV)
26	Cu-63 (n, $\alpha$ ) Cu-60	54	Delta energy (MeV)
27	Cu-65 (n,2n) Cu-64	55	Delta lethargy
28	In-115 (n,n') In-115m		

**Table 3-6**  
**Row positions of response functions in tables 7002 and 7004**

Row	Response
1	Pu-238 (n,fission)
2	U-234 neutrons/fission (nubar)
3	U-235 neutrons/fission (nubar)
4	U-236 neutrons/fission (nubar)
5	U-238 neutrons/fission (nubar)
6	Pu-238 neutrons/fission (nubar)
7	Pu-239 neutrons/fission (nubar)
8	Pu-240 neutrons/fission (nubar)
9	Pu-241 neutrons/fission (nubar)
10	Pu-242 neutrons/fission (nubar)
11	U-234 fission spectrum (chi)
12	U-236 fission spectrum (chi)
13	Pu-238 fission spectrum (chi)
14	Pu-240 fission spectrum (chi)
15	Pu-241 fission spectrum (chi)
16	Pu-242 fission spectrum (chi)

The response function tables are identified in the RAMA nuclear data library with the nuclide identifiers 7001, 7002, 7003, and 7004. Response tables 7001 (Part A) and 7002 (Part B) contain response functions which have a flat weighting corresponding to the in-vessel surveillance capsule location. Response tables 7003 (Part A) and 7004 (Part B) contain response functions which have a weighting corresponding to the 1/4T location in the pressure vessel.

### 3.4 Surveillance Capsule Activation Results

In accordance with the Safety Evaluation Report issued by the U.S. Nuclear Regulatory Commission [13] for application of RAMA to BWR capsule and RPV fluence evaluations, the evaluation should contain a comparison of predicted capsule activations to reported measurements of specific activities. This section addresses the evaluation of the Monticello surveillance program flux wires and the comparison to measurements.

Copper, iron, and nickel flux wires were irradiated in the Monticello surveillance capsule at the 300° azimuth during the first 23 cycles of operation. The wires were removed after being irradiated for a total of 28.2 EFPY. Activation measurements were performed following irradiation for the following reactions [see Appendix A]:  $^{63}\text{Cu} (n, \alpha) ^{60}\text{Co}$ ,  $^{54}\text{Fe} (n,p) ^{54}\text{Mn}$ , and  $^{58}\text{Ni} (n,p) ^{58}\text{Co}$ .

Table 3-7 provides a comparison of the RAMA calculated specific activities and the measured specific activities for the surveillance capsule flux wire specimens. The C/M results show good agreement between the RAMA calculated values and the measured values. The cycle 23 flux wire average C/M value is 1.03 with a standard deviation of  $\pm 0.11$ . The average C/M value for the copper flux wires is 0.89 with a standard deviation of  $\pm 0.04$ , for the iron flux wires is 1.08 with a standard deviation of  $\pm 0.03$  and for the nickel flux wires is 1.13 with a standard deviation of  $\pm 0.03$ .

**Table 3-7**  
**Comparison of specific activities for Monticello 300° surveillance capsule flux wires (c/m)**

Flux Wires	Measured (dps/mg)	Calculated (dps/mg)	Calculated vs. Measured	Standard Deviation
<b>Copper</b>				
P4	14.07	12.94	0.92	
P5	13.53	12.28	0.91	
P9	15.77	12.97	0.82	
P10	14.67	13.22	0.90	
<b>Average</b>	<b>14.51</b>	<b>12.85</b>	<b>0.89</b>	<b><math>\pm 0.04</math></b>
<b>Iron</b>				
P4	81.49	90.45	1.11	
P5	80.79	86.74	1.07	
P9	90.01	93.19	1.04	
P10	85.55	93.03	1.09	
<b>Average</b>	<b>84.46</b>	<b>90.85</b>	<b>1.08</b>	<b><math>\pm 0.03</math></b>
<b>Nickel</b>				
P4	981.0	1155.0	1.18	
P5	968.8	1084.0	1.12	
P9	1141.0	1251.0	1.10	
P10	1071.0	1222.0	1.14	
<b>Average</b>	<b>1040.0</b>	<b>1178.0</b>	<b>1.13</b>	<b><math>\pm 0.03</math></b>
<b>Total Flux Wire Average</b>	<b>—</b>	<b>—</b>	<b>1.03</b>	<b><math>\pm 0.11</math></b>

The average C/M results for the flux wires in each specimen packet are listed in Table 3-8.

**Table 3-8**  
**Average comparison of specific activities for Monticello 300° surveillance capsule flux wires by specimen packet**

Packet Identifier	Calculated vs. Measured Average	Standard Deviation
P4	1.07	±0.13
P5	1.03	±0.11
P9	0.98	±0.14
P10	1.04	±0.13

### 3.5 Surveillance Capsule Fluence Results

Table 3-9 shows the calculated best estimate >1.0 MeV neutron fluence for the Monticello 300° capsule specimen locations at 28.2 EFPY. No bias is applied, as indicated above.

**Table 3-9**  
**Best estimate >1.0 MeV neutron fluence in Monticello 300° ISP capsule specimen packets**

Specimen Packet	Best Estimate Fluence (n/cm <sup>2</sup> )
P4	8.97E+17
P5	8.69E+17
P9	9.14E+17
P10	9.10E+17
<b>Average</b>	<b>8.98E+17</b>

# 4

## CHARPY TEST DATA

---

### 4.1 Charpy Test Procedure

Charpy impact tests were conducted in accordance with ASTM Standards E185-82 and E23-02. The 1982 version of E185 has been reviewed and approved by NRC for surveillance capsule testing applications. This standard references ASTM E23. The tests were conducted using a Tinius Olsen Testing Machine Company, Inc. Model 84 impact test machine with a 300 ft-lb (406.75 J) range. The Model 84 is equipped with a dial gage as well as the MPM optical encoder system for accurate absorbed energy measurement. The machine is also equipped with an instrumented striker, so a total of three independent measurements of the absorbed energy were made for every test. In all cases, the optical encoder measured energy was reported as the impact energy. The optical encoder energy is much more accurate than the dial. The optical encoder can resolve the energy to within 0.04 ft-lbs (0.054 J), whereas, for the dial, the resolution is around 0.25 ft-lbs (0.34 J). The impact energy was corrected for windage and friction for each test performed. The velocity of the striker at impact was nominally 18 ft/s (5.49 m/s). The MPM encoder system measures the exact impact velocity for every test. Calibration of the machine was verified as specified in E23 and verification specimens were provided by NIST.

The E23 procedure for specimen temperature control using an in-situ heating and cooling system was followed. The advantage of using the MPM in-situ heating/cooling technology is that each specimen is thermally conditioned right up to the instant of impact. Thermal losses, such as those associated with liquid bath systems, are completely eliminated. Each specimen was held at the desired test temperature for at least 5 minutes prior to testing and the fracture process zone temperature was held to within  $\pm 1.8$  F ( $\pm 1$  C) up to the instant of strike. Precision calibrated tongs were used for specimen centering on the test machine.

Lateral expansion (LE) was determined from measurements made with a lateral expansion gage. The lateral expansion gage was calibrated using precision gage blocks which are traceable to NIST. The percentage of shear fracture area was determined by integrating the ductile and brittle fracture areas using the MPM image analysis system.

The number of Charpy specimens for measurement of the transition region and upper shelf was limited. Therefore, the choice of test temperatures was very important. Prior to testing, the Charpy energy-temperature curve was predicted using embrittlement models and previous data. The first test was then conducted near the middle of the transition region and test temperature decisions were then made based on the test results. Overall, the goal was to perform at least three tests on the upper shelf and to use the remaining specimens to characterize the 30 ft-lb (41 J) index. This approach was successful as illustrated below.

## 4.2 Charpy Test Data

A total of 14 irradiated base metal specimens were tested over the transition region temperature range and on the upper shelf. The data are summarized in Table 4-1. The C2220 base metal surveillance specimens have an LT orientation. In addition to the energy absorbed by the specimen during impact, the measured lateral expansion values and the percentage shear fracture area for each test specimen are listed in the tables. The Charpy energy was read from the optical encoder and has been corrected for windage and friction in accordance with ASTM E23. The impact energy is the energy required to initiate and propagate a crack. The optical encoder and the dial cannot correct for tossing energy and therefore this small amount of additional energy, if present, may be included in the data for some tests.

**Table 4-1**  
Charpy V-notch impact test results for base metal specimens from the Monticello 300 surveillance capsule

Specimen Identification	Test Temperature °F (°C)	Impact Energy ft-lb (J)	Fracture Appearance (% Shear Area)	Lateral Expansion mils (mm)
JDM	20.0 (-6.7)	12.75 (17.28)	11.4	9.0 (0.2)
JD3	40.6 (4.8)	11.30 (15.32)	15.5	10.0 (0.3)
D14	71.6 (22.0)	16.44 (22.29)	22.4	18.5 (0.5)
JDD	95.8 (35.4)	30.99 (42.02)	24.1	28.5 (0.7)
JDT	119.2 (48.5)	31.04 (42.08)	30.4	28.0 (0.7)
D3K	132.9 (56.1)	67.62 (91.69)	52.0	58.0 (1.5)
JD2	148.7 (64.8)	58.04 (78.69)	43.2	50.5 (1.3)
D1B	164.3 (73.5)	76.15 (103.24)	62.9	64.0 (1.6)
JDP	177.3 (80.7)	61.90 (83.93)	61.1	51.5 (1.3)
D1M	192.6 (89.2)	108.84 (147.57)	89.0	81.5 (2.1)
D3J	213.6 (100.9)	108.62 (147.27)	100.0	81.0 (2.1)
D1K	249.4 (120.8)	108.01 (146.44)	100.0	86.0 (2.2)
D1J	287.4 (141.9)	118.79 (161.06)	100.0	86.0 (2.2)
D3B	409.5 (209.7)	107.51 (145.76)	100.0	78.5 (2.0)

The lateral expansion is a measure of the transverse plastic deformation produced by the striking edge of the striker during the impact event. Lateral expansion is determined by measuring the maximum change of specimen thickness along the sides of the specimen. Lateral expansion is a measure of the ductility of the specimen. The nuclear industry tracks the embrittlement shift using the 35 mil (0.89 mm) lateral expansion index. In accordance with ASTM E23, the lateral expansion for some specimens, which could be broken after the impact test, should not be

reported as broken since the lateral expansion of the unbroken specimen is less than that for the broken specimen. Therefore, when these conditions exist, the value listed is the unbroken measurement and a footnote is included to identify these specimens. All of the 300° capsule specimens that did not separate during the test could be broken by hand under the ASTM E23 requirements.

The percentage of shear fracture area is a direct quantification of the transition in the fracture modes as the temperature increases. All metals with a body centered cubic lattice structure, such as ferritic pressure vessel materials, undergo a transition in fracture modes. At low test temperatures, a crack propagates in a brittle manner and cleaves across the grains. As the temperature increases, the percentage of shear (or ductile) fracture increases. This temperature range is referred to as the transition region and the fracture process is mixed mode. As the temperature increases further, the fracture process is eventually completely ductile (i.e., no brittle component) and this temperature range is referred to as the upper shelf region.

Preparation of P-T operating curves requires the determination of the Charpy 30 ft-lb (41 J) transition temperature shift. This index is determined by fitting the energy-temperature data to find the mean curve. It is also necessary to estimate the upper shelf energy to ensure that the shelf has not dropped below the 10CFR50, Appendix G, 50 ft-lb (67.8 J) screening criterion. The Charpy data analysis results are provided in the next section of this report.

# 5

## CHARPY TEST RESULTS

---

### 5.1 Analysis of Impact Test Results

For analysis of the Charpy test data, the BWRVIP ISP has selected the hyperbolic tangent (tanh) function as the statistical curve-fit tool to model the transition temperature toughness data. A hyperbolic tangent curve-fitting program named CVGRAPH [10], developed by ATI Consulting, was used to fit the Charpy V-notch energy and lateral expansion data. Analysis methodology (e.g., definition of upper fixed shelf and lower shelf) followed the BWRVIP conventions established for analysis of all ISP data [19]. The impact energy curve-fits from CVGRAPH are provided in Figures 5-1 (CVN energy) and 5-2 (lateral expansion).

For the analysis of Charpy energy test data (Figure 5-1), lower shelf energy was fixed at 2.5 ft-lbs (3.4 J). Upper shelf energy was fixed at the average of all test energies (at least 3) exhibiting shear greater than or equal to 95%, consistent with ASTM Standard E185-82 [3]. For analysis of the lateral expansion test data (Figure 5-2), the lower shelf was fixed at 1.0 mils; the fixed upper shelf was defined as the average of the lateral expansion test data points at the same test temperatures used to define the fixed upper shelf energy.

### 5.2 Irradiated Versus Unirradiated CVN Properties

Table 5-1 summarizes the  $T_{30}$  [30 ft-lb (41 J) Transition Temperature],  $T_{35\text{mil}}$  [35 mil (0.89 mm) Lateral Expansion Temperature],  $T_{50}$  [50 ft-lb (68 J) Transition Temperature], and Upper Shelf Energy for the unirradiated and irradiated material and shows the change (shift) from baseline values. The unirradiated values of  $T_{30}$  and  $T_{50}$  were taken from the CVGRAPH fit provided in Figure 2-1; the unirradiated value of  $T_{35\text{mil}}$  was previously determined in [19]. The irradiated values are from the index temperatures determined in Figures 5-1 and 5-2.

Table 5-2 provides a comparison of the measured shift to predicted shift. Predicted shift is based on the formula provided in Reg. Guide 1.99 Rev. 2 [5] and shown in Note 2 to the table. The fluence was input as  $9.05 \text{ E } +17 \text{ n/cm}^2$ , which is the rounded average of the fluences reported in Section 3.5 for Packets 4 and Packets 9 (the two packets containing the base metal Charpy specimens). The measured shift is within the value expected (e.g., the measured shift is less than predicted shift + margin).

Measured percent decrease in USE is presented in Table 5-3 and compared to the percent decrease predicted by Figure 2 of Reg. Guide 1.99 Rev. 2. The observed drop in USE is slightly greater than predicted.

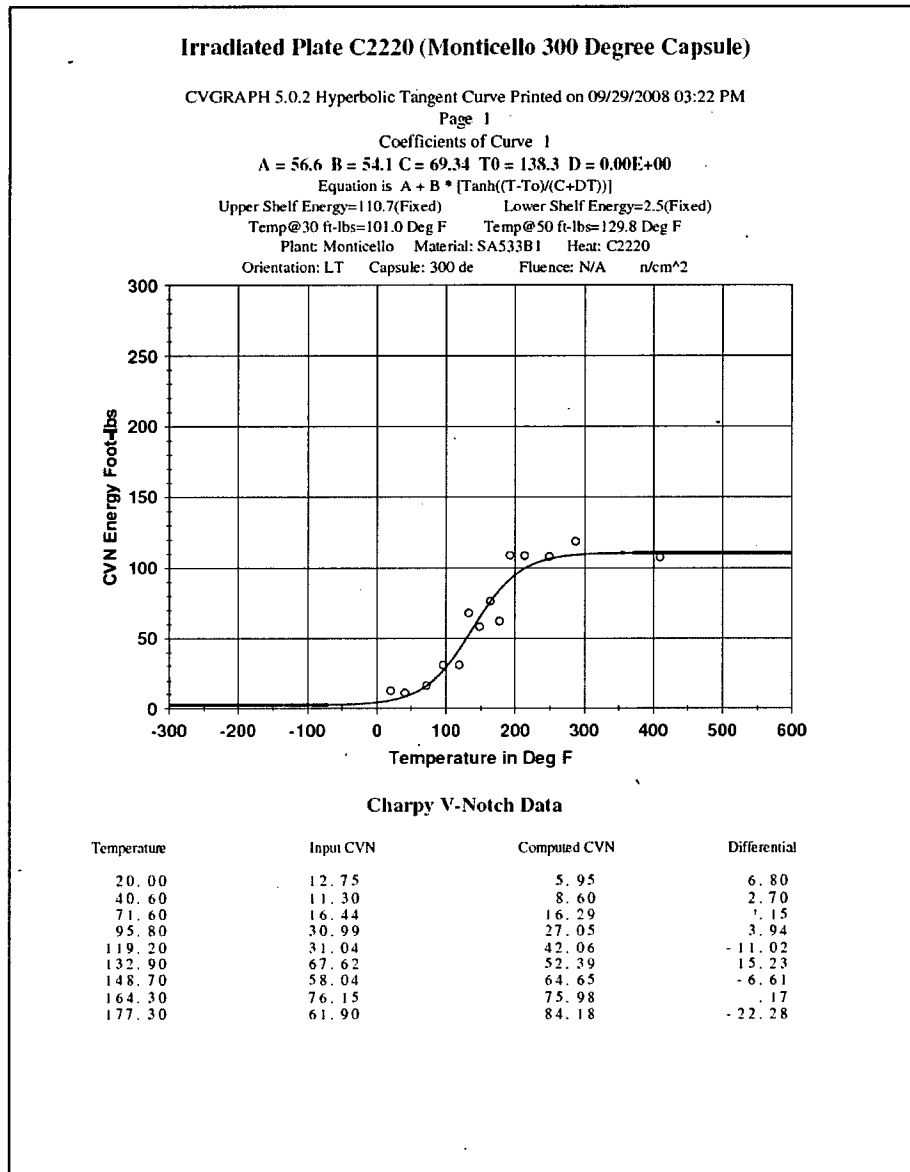


**Figure 5-1**  
Irradiated plate C2220 (Monticello 300° capsule) Charpy energy plot

**Irradiated Plate C2220 (Monticello 300 Degree Capsule)**

Page 2

Plant: Monticello Material: SA533B1 Heat: C2220  
Orientation: LT Capsule: 300 de Fluence: N/A n/cm<sup>2</sup>**Charpy V-Notch Data**

Temperature	Input CVN	Computed CVN	Differential
192.60	108.84	92.01	16.83
213.60	108.62	99.63	8.99
249.40	108.01	106.48	1.53
287.40	118.79	109.25	9.54
409.50	107.51	110.66	-3.15

Correlation Coefficient = .966

**Figure 5-1 (continued)**  
**Irradiated plate C2220 (Monticello 300° capsule) Charpy energy plot**

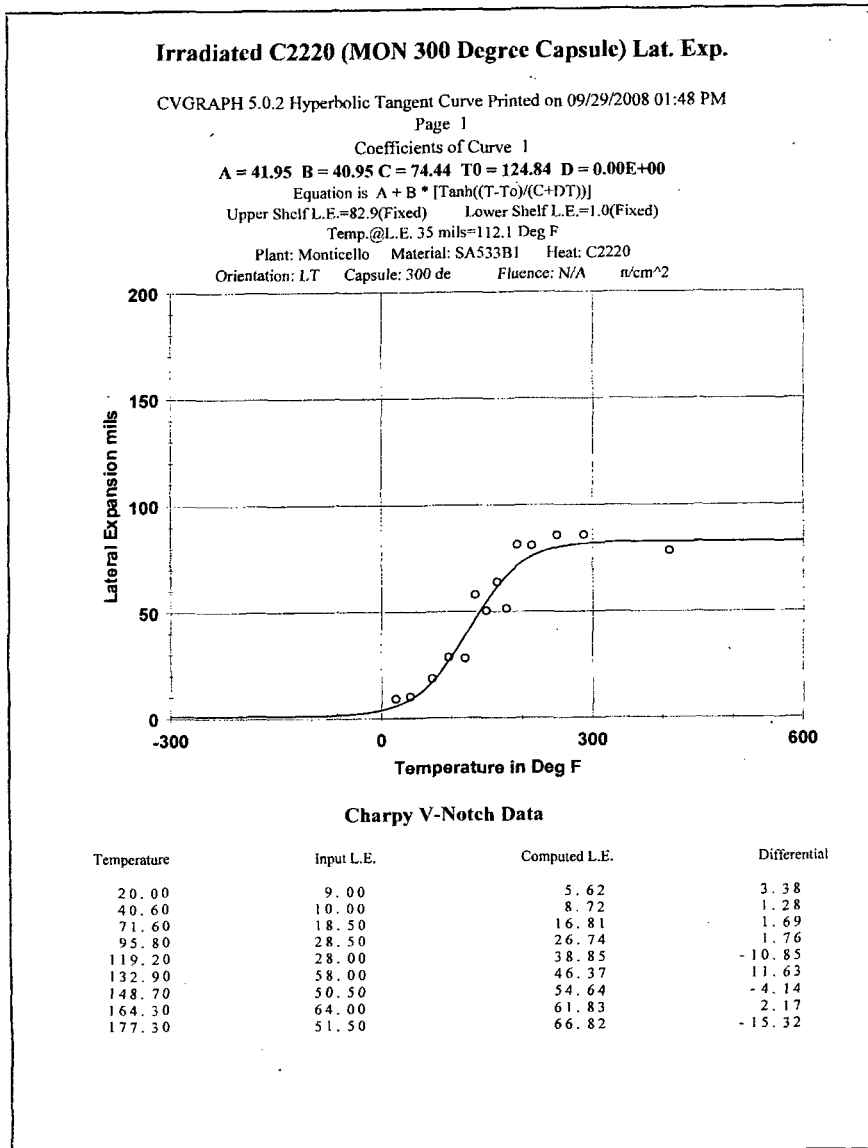


**Figure 5-2**  
 Irradiated plate C2220 (Monticello 300° capsule) lateral expansion plot

**Irradiated C2220 (MON 300 Degree Capsule) Lat. Exp.**

Page 2

Plant: Monticello Material: SA533B1 Heat: C2220  
Orientation: LT Capsule: 300 de Fluence: N/A n/cm<sup>2</sup>

**Charpy V-Notch Data**

Temperature	Input L.E.	Computed L.E.	Differential
192.60	81.50	71.48	10.02
213.60	81.00	75.99	5.01
249.40	86.00	80.11	5.89
287.40	86.00	81.87	4.13
409.50	78.50	82.86	-4.36

Correlation Coefficient = .966

**Figure 5-2 (continued)**  
**Irradiated plate C2220 (Monticello 300° capsule) lateral expansion plot**

Charpy Test Results

**Table 5-1**  
Effect of irradiation (E>1.0 MeV) on the notch toughness properties of plate heat C2220

Material Identity	T <sub>30</sub> , 30 ft-lb (41 J) Transition Temperature			T <sub>35mil</sub> , 35 mil (0.89 mm) Lateral Expansion Temperature			T <sub>50</sub> , 50 ft-lb (68 J) Transition Temperature			CVN Upper Shelf Energy (USE)		
	Unirrad °F (°C)	Irradiated °F (°C)	ΔT <sub>30</sub> °F (°C)	Unirrad °F (°C)	Irradiated °F (°C)	ΔT <sub>35mil</sub> °F (°C)	Unirrad °F (°C)	Irradiated °F (°C)	ΔT <sub>50</sub> °F (°C)	Unirrad ft-lb (J)	Irradiated ft-lb (J)	Change ft-lb (J)
C2220 (LT orientation)	25.8 (-3.4)	101.0 (38.3)	75.2 (41.8)	40.7 (4.8)	112.1 (44.5)	71.4 (39.7)	48.6 (9.2)	129.8 (54.3)	81.2 (45.1)	132.4 (179.5)	110.7 (150.1)	-21.7 (-29.4)

**Table 5-2**  
Comparison of actual versus predicted embrittlement

Identity	Material	Fluence (x10 <sup>17</sup> n/cm <sup>2</sup> )	Measured Shift <sup>1</sup> °F (°C)	RG 1.99 Rev. 2 Predicted Shift <sup>2</sup> °F (°C)	RG 1.99 Rev. 2 Predicted Shift+Margin <sup>2,3</sup> °F (°C)
C2220	Monticello Plate (SA533B-1) (LT orientation)	9.05	75.2 (41.8)	47.3 (26.3)	81.3 (45.2)

Notes:

1. See Table 5-1, ΔT<sub>30</sub>.
2. Predicted shift = CF × FF, where CF is a Chemistry Factor taken from tables from USNRC Reg. Guide 1.99, Rev. 2 [5], based on the material's Cu/Ni content, and FF is Fluence Factor,  $f^{0.28-0.10 \log f}$ , where f = fluence (E > 1.0 MeV) specified.
3. Margin Term is defined as 34°F for plate materials and 56°F for weld materials, or margin equals shift (whichever is less), per Reg. Guide 1.99, Rev. 2 [5].

**Table 5-3**  
**Percent decrease in Upper Shelf Energy (USE)**

Identity	Material	Fluence ( $\times 10^{17}$ n/cm <sup>2</sup> )	Cu Content (wt%)	Measured Decrease in USE <sup>1</sup> (%)	Predicted Decrease in USE <sup>2</sup> (%)
C2220	Monticello Plate (SA533B-1)	9.05	0.16	16.4	14

Notes:

1. Calculated from Table 5-1, (Change/Unirradiated) \* 100. A positive number indicates a decrease in USE; a negative number indicates the USE increased over the unirradiated value.
2. Based on extrapolation of and interpolation between the curves given in Figure 2 of Reg. Guide 1.99 Rev. 2 [5].

# 6

## REFERENCES

---

1. 10 CFR 50, Appendices G (*Fracture Toughness Requirements*) and H (*Reactor Vessel Material Surveillance Program Requirements*), Federal Register, Volume 60, No. 243, dated December 19, 1995.
2. *Fracture Toughness Criteria for Protection Against Failure*, Appendix G to Section III or XI of the ASME Boiler & Pressure Vessel Code, 1995 Edition with addenda through 1996 Addenda.
3. ASTM E185-82, *Standard Practice for Conducting Surveillance Tests for Light-Water Cooled Nuclear Power Reactor Vessels*, E706 (IF), ASTM Standards, Section 3, American Society for Testing and Materials, Philadelphia, PA, 1993.
4. BWRVIP-86-A: BWR Vessel and Internals Project, Updated BWR Integrated Surveillance Program Implementation Plan. EPRI, October 2002. Technical Report 1003346.
5. U.S. NRC Regulatory Guide 1.99, "Radiation Embrittlement of Reactor Vessel Materials," Revision 2, May 1988.
6. "Examination, Testing, and Evaluation of Irradiated Pressure Vessel Surveillance Specimens from the Monticello Nuclear Generating Plant," L.M. Lowry, M.P. Landow, J.S. Perrin, A.M. Walters, R.G. Jung, and R.S. Denning, Battelle Columbus Laboratories, BCL-585-84-2, Revision 1, November 5, 1984.
7. Structural Integrity Associates, "Review of the Test Results of Two Surveillance Capsules, and Recommendations for the Materials Properties and Pressure-Temperature Curves to be used for the Monticello Reactor Pressure Vessel", SIR-97-003, October, 1998.
8. NUREG-CR-6426, ORNL-6892/V2, Volume 2, *Ductile Fracture Toughness of Modified A302 Grade B Plate Materials*, D.E. McCabe, E.T. Manneschimdt, and R.L. Swain, Oak Ridge National Laboratory.
9. "Monticello Nuclear Generating Station Information on Reactor Vessel Material Surveillance Program," General Electric Company, NEDO-24197, 79NED297, June 1979.
10. CVGRAPH, Hyperbolic Tangent Curve Fitting Program, Developed by ATI Consulting, Version 5.0.2, Revision 1, 3/26/02.
11. "Calculational and Dosimetry Methods for Determining Pressure Vessel Neutron Fluence," Nuclear Regulatory Commission Regulatory Guide 1.190, March 2001.
12. BWRVIP-126: BWR Vessel Internals Project, RAMA Fluence Methodology Software, Version 1.0. EPRI, Palo Alto, CA: 2003. 1007823.
13. Letter from William H. Bateman (U.S. NRC) to Bill Eaton (BWRVIP), Safety Evaluation of Proprietary EPRI Reports BWRVIP-114, -115, -117, and -121 and TWE-PSE-001-R-001. dated May 13, 2005.

---

*References*

14. Letter from Matthew A. Mitchell (U.S. NRC) to Rick Libra (BWRVIP), "Safety Evaluation of Proprietary EPRI Report BWR Vessel and Internals Project, Evaluation of Susquehanna Unit 2 Top Guide and Core Shroud Material Samples Using RAMA Fluence Methodology (BWRVIP-145)," dated February 7, 2008.
15. BWRVIP-189: BWR Vessel and Internals Project, Evaluation of RAMA Fluence Methodology Computational Uncertainty. EPRI, Palo Alto, CA: 2008. 1016938.
16. "BUGLE-96: Coupled 47 Neutron, 20 Gamma-Ray Group Cross Section Library Derived from ENDF/B-VI for LWR Shielding and Pressure Vessel Dosimetry Applications," RSICC Data Library Collection, DLC-185, March 1996.
17. BWRVIP-114: BWR Vessel Internals Project, RAMA Fluence Methodology Theory Manual. EPRI, Palo Alto, CA: 2003. 1003660.
18. BWRVIP-121: BWR Vessel Internals Project, RAMA Fluence Methodology Procedures Manual. EPRI, Palo Alto, CA: 2003. 1008062.
19. BWRVIP-135, Revision 1: BWR Vessel and Internal Project Integrated Surveillance Program (ISP) Data Source Book and Plant Evaluations. EPRI, Palo Alto, CA: 2007. 1013400.

# A

## APPENDIX A – DOSIMETER ANALYSIS

---

### A.1 Dosimeter Material Description

The primary dosimeter materials are pure metal wires which were located within the surveillance capsule. The wire types provided for the capsule surveillance program are copper, iron, and nickel. Each wire is about 3 inches (7.62 cm) long.

### A.2 Dosimeter Cleaning and Mass Measurement

Upon receipt at the radiometric lab, the wires were visually inspected and cleaned with a lab wipe soaked in pure ethanol. The wire segments were then examined under a low magnification optical microscope. There appeared to be evidence of oxidation and some remaining surface contamination, indicating the need for further cleaning. This was accomplished by soaking the wire segments in a 4N solution of hydrochloric acid, followed by immersion in a 2N solution of nitric acid. The wires were then rinsed with distilled water, wiped once more with ethanol, and then allowed to dry in air at room temperature. The wires then exhibited a clean, shiny appearance. To illustrate the cleaning and coiling procedure, Figures A-1 through A-9 show low-power magnifications of the Charpy packet 10 (P10) wires as they were found prior to cleaning, after cleaning, and after coiling. In general, iron and copper exhibited the most oxidation, while the nickel wires were relatively clean.



**Figure A-1**  
P10-Cu dosimeter wire prior to cleaning



**Figure A-2**  
P10-Cu dosimeter wire after cleaning

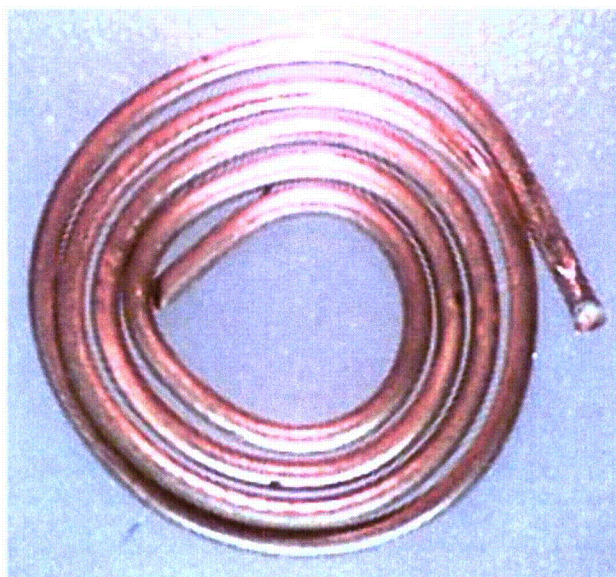


**Figure A-3**  
P10-Cu dosimeter after cleaning and coiling



**Figure A-4**  
P10-Fe dosimeter wire prior to cleaning

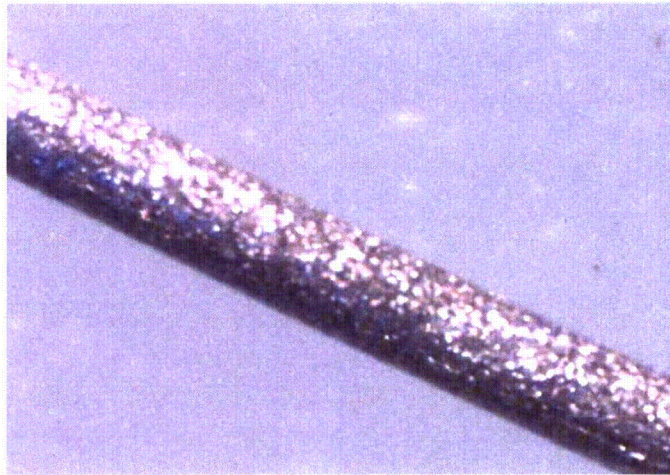


**Figure A-5**  
P10-Fe dosimeter wire after cleaning



**Figure A-6**  
P10-Fe dosimeter after cleaning and coiling

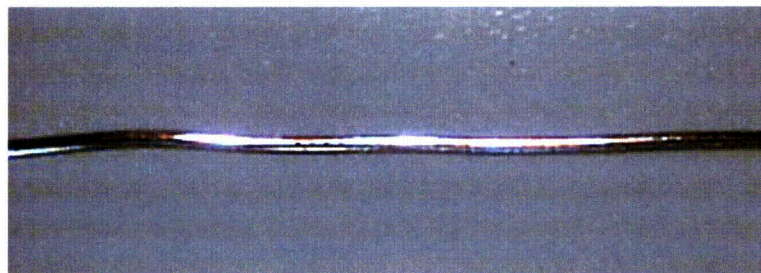


**Figure A-7**  
P10-Ni dosimeter wire prior to cleaning

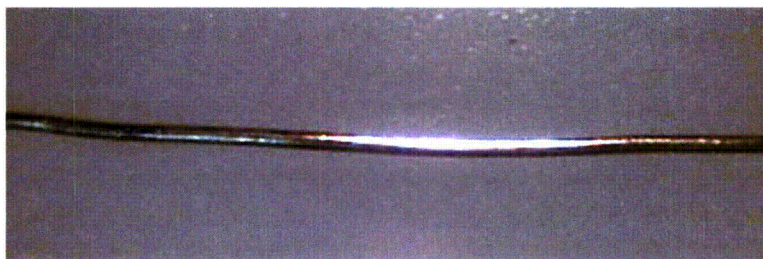


**Figure A-8**  
P10-Ni dosimeter wire after cleaning



**Figure A-9**  
P10-Ni dosimeter after cleaning and coiling

The total mass of each wire was measured using a Mettler AX-205 digital balance. Table A-1 lists the results of these measurements, as well as the identification assigned to each dosimeter. Each wire was wrapped around a thin metal rod to form a coil of approximately 0.5 inch (12.7 mm) diameter, which yields a reasonable approximation to a point source geometry at the distance the dosimeter wires are placed from the gamma detector. The coiled wire segments were pressed firmly against a hard surface to flatten the coil.

**Table A-1**  
**Wire dosimeter masses**

Wire Dosimeter ID	Mass (mg)
P4-Cu	386.77
P4-Fe	124.13
P4-Ni	264.67
P5-Cu	324.75
P5-Fe	135.02
P5-Ni	278.41
P9-Cu	398.68
P9-Fe	69.44
P9-Ni	317.29
P10-Cu	507.41
P10-Fe	148.45
P10-Ni	351.67

### **A.3 Radiometric Analysis**

Radiometric analysis was performed using high resolution gamma emission spectroscopy. In this method, gamma emissions from the dosimeter materials are detected and quantified using solid-state gamma ray detectors and computer-based signal processing and spectrum analysis. The specifications of the gamma ray spectrometer system (GRSS) are listed in Table A-2. While the overall GRSS features three separate hyper pure germanium (HPGe) detectors, only one was used for this study. The detector is housed in a lead-copper shield (cave) to reduce background count rates.

**Table A-2**  
**GRSS specifications**

System Component	Description and/or Specifications
Detector	Canberra Model GC1420 HPGe
Energy Resolution	1.77 KeV @ 1332.5 KeV
Detector Efficiency (relative to a 3 inch x 3 inch (7.62 cm x 7.62 cm)NaI crystal)	14% at 1332.5 KeV
Amplifier	Aptec Nuclear Inc. Model 6300 Low-Noise Spectroscopy Amplifier
ADC	Aptec Nuclear Inc. Model S5008 PC-ISA card, 8192 Channels, 6 $\mu$ sec. fixed conversion time, successive approximation conversion method
Computer System	1.6 GHZ Pentium 4-Based PC, 2 GB Main Memory, 500 GB Hard Disk, 42-inch Monitor, Lexmark T644 Printer
Software	Aptec Nuclear Inc. OSQ/Professional Version 7.08
Bias Voltage Supply	Mechtronics Model 258

System calibration was performed using a National Institute for Standards and Technology (NIST) traceable quasi-point source supplied by QSA Global Corporation. The analysis software was procured from Aptec Nuclear, Inc. and provides the capability for energy resolution and efficiency calibration using specified standard source information. Calibration information is stored on magnetic disk for use by the spectrographic analysis software package.

Since detector efficiency depends on the source-detector geometry, a fixed, reproducible geometry/distance must be selected for the gamma spectrographic analysis of the dosimeter materials. For the dosimeter wires, the counting geometry was that of a quasi-point source (coiled wire) placed 5 inches (12.7 cm) vertically from the top surface of the detector shell. In this way, extended sources up to 0.5 inch (1.27 cm) can be analyzed with a good approximation to a point source. The coiled wires were well within the area needed to approximate a point source geometry. The HPGe detector was calibrated for efficiency using the NIST traceable source.

The accuracy of the efficiency calibration was checked using a gamma spectrographic analysis of a NIST traceable gamma source, separate from that used to perform the efficiency calibration, and supplied by a separate vendor. The isotope contained in this check source emits gamma rays which span the energy response of the detector for the dosimeter materials. These measurements show that the efficiency calibration is providing a valid estimate of source activity. The acceptance criteria for these measurements are that the software must yield a valid isotopic identification, and that the quantified activity of each correctly identified isotope must be within the uncertainty specified in the source certification. Validation of system performance using traceable check sources was performed prior to starting the counting tasks, and upon completion

of all counting. The counting system performance was acceptable in each case, indicating that the counting system properties did not change during the course of the counting procedure.

Table A-3 shows the counting schedule established for this work. There was no requirement for order of counting, since the dosimeter materials still contained sufficient quantities of activation products to allow accurate radio assay. Counting times were sufficient to achieve the desired statistical accuracy for gamma emissions of interest in all cases.

**Table A-3**  
**Counting schedule for the dosimeter materials**

Dosimeter ID	Count Start Date	Count Start Time (ET)	Count Duration (Live Time Seconds)
P4-Cu	5/19/08	17:14	59912
P4-Fe	5/20/08	9:55	89883
P4-Ni	5/21/08	10:56	19253
P5-Cu	5/22/08	9:27	89115
P5-Fe	5/21/08	16:31	58646
P5-Ni	5/23/08	10:14	20203
P9-Cu	5/23/08	15:57	345544
P9-Fe	5/27/08	16:26	75966
P9-Ni	5/28/08	13:36	71471
P10-Cu	5/29/08	10:06	24648
P10-Fe	5/29/08	16:59	61257
P10-Ni	5/30/08	17:12	230009

Neutrons interact with the constituent nuclei of the dosimeter materials, producing radionuclides in varying amounts depending on total neutron fluence and its energy spectrum, and the nuclear properties of the dosimeter materials. Table A-4 lists the reactions of interest and their resultant radionuclide products for each element contained in the dosimeters. These are threshold reactions involving an n-p or n- $\alpha$  interaction.

**Table A-4**  
**Neutron-induced reactions of interest**

Dosimeter Material	Neutron-Induced Reaction	Reaction Product Radionuclide
Iron	$\text{Fe}^{54}(\text{n,p})\text{Mn}^{54}$	$\text{Mn}^{54}$
Copper	$\text{Cu}^{63}(\text{n},\alpha)\text{Co}^{60}$	$\text{Co}^{60}$
Nickel	$\text{Ni}^{58}(\text{n,p})\text{Co}^{58}$	$\text{Co}^{58}$

Finally, Table A-5 presents the primary results of interest for flux determination. The activity units are in dps/mg, which normalizes the activity to dosimeter mass. The activities are specified for both the time of the analysis, and a reference date/time, which in this case is the Monticello shutdown date and time. This was specified as March 14, 2007, at 0:00 EST.

**Table A-5**  
**Results of the radiometric analysis**

Dosimeter ID	Isotope ID	Activity at Count Date/Time (dps/mg)	Activity at Reference Date/Time <sup>a</sup> (dps/mg)	Activity Uncertainty (%)
P4-Cu	<sup>60</sup> Co	12.07	14.07	1.78
P4-Fe	<sup>54</sup> Mn	31.13	81.49	1.99
P4-Ni	<sup>58</sup> Co	13.95	981.0	2.42
P5-Cu	<sup>60</sup> Co	11.57	13.53	1.74
P5-Fe	<sup>54</sup> Mn	30.78	80.79	2.01
P5-Ni	<sup>58</sup> Co	13.49	968.8	2.44
P9-Cu	<sup>60</sup> Co	13.48	15.77	1.69
P9-Fe	<sup>54</sup> Mn	33.83	90.01	2.03
P9-Ni	<sup>58</sup> Co	15.18	1141	2.08
P10-Cu	<sup>60</sup> Co	12.51	14.67	1.80
P10-Fe	<sup>54</sup> Mn	32.02	85.55	2.00
P10-Ni	<sup>58</sup> Co	13.95	1071	2.01

<sup>a</sup> March 14, 2007 at 0:00 EST is the reference date and time.

### **Export Control Restrictions**

Access to and use of EPRI Intellectual Property is granted with the specific understanding and requirement that responsibility for ensuring full compliance with all applicable U.S. and foreign export laws and regulations is being undertaken by you and your company. This includes an obligation to ensure that any individual receiving access hereunder who is not a U.S. citizen or permanent U.S. resident is permitted access under applicable U.S. and foreign export laws and regulations. In the event you are uncertain whether you or your company may lawfully obtain access to this EPRI Intellectual Property, you acknowledge that it is your obligation to consult with your company's legal counsel to determine whether this access is lawful. Although EPRI may make available on a case-by-case basis an informal assessment of the applicable U.S. export classification for specific EPRI Intellectual Property, you and your company acknowledge that this assessment is solely for informational purposes and not for reliance purposes. You and your company acknowledge that it is still the obligation of you and your company to make your own assessment of the applicable U.S. export classification and ensure compliance accordingly. You and your company understand and acknowledge your obligations to make a prompt report to EPRI and the appropriate authorities regarding any access to or use of EPRI Intellectual Property hereunder that may be in violation of applicable U.S. or foreign export laws or regulations.

**The Electric Power Research Institute (EPRI)**, with major locations in Palo Alto, California; Charlotte, North Carolina; and Knoxville, Tennessee, was established in 1973 as an independent, nonprofit center for public interest energy and environmental research. EPRI brings together members, participants, the Institute's scientists and engineers, and other leading experts to work collaboratively on solutions to the challenges of electric power. These solutions span nearly every area of electricity generation, delivery, and use, including health, safety, and environment. EPRI's members represent over 90% of the electricity generated in the United States. International participation represents nearly 15% of EPRI's total research, development, and demonstration program.

Together...Shaping the Future of Electricity

### **Program:**

Nuclear Power

© 2010 Electric Power Research Institute (EPRI), Inc. All rights reserved. Electric Power Research Institute, EPRI, and TOGETHER...SHAPING THE FUTURE OF ELECTRICITY are registered service marks of the Electric Power Research Institute, Inc.

1021557

### **Electric Power Research Institute**

3420 Hillview Avenue, Palo Alto, California 94304-1338 • PO Box 10412, Palo Alto, California 94303-0813 USA  
800.313.3774 • 650.855.2121 • [askepri@epri.com](mailto:askepri@epri.com) • [www.epri.com](http://www.epri.com)